30mmHgを超えると脳血流が減少するとされている．イヌを用いて硬膜外腔圧と脳脊髄液圧との関係を調べた文献によると，硬膜外腔に生食を注入し硬膜外腔圧を上昇させていくと，それに伴い脳脊髄液圧も上昇し，脳脊髄液圧は硬膜外腔圧の90％程度の値を示した[2]．このことから，エピドラスコピー時に頚部硬膜外腔圧が80mmHg程度になると脳脊髄液圧も70mmHg程度になっていると推測され，脳血流減少や静脈系の圧迫による組織血流の停滞が生じる．この状態が持続すると上記のような危機的な合併症につながると考えられる．

このような頚部硬膜外腔圧上昇を予防するためには，カテーテルシャフトによる癒着剥離を優先し，できるかぎり生食の急激な注入を避け，総使用量も減少させるようにすることが重要である．また，適切な鎮静を施すことで，癒着剥離時の痛みに伴うスパイク状の圧上昇を予防することが可能となる．また，頚部硬膜外腔圧をモニタリングしながらエピドラスコピーを行うことで，圧上昇を回避でき，合併症の予防につながる．しかし，特に癒着剥離後の洗浄で頭痛などの症状が出現した場合は，硬膜外腔からの生食の排泄経路に問題がなければ生食注入を中止後1～2分で圧は元のレベルに戻るので，時間を空けて間欠的に生食注入を行うべきである．

エピドラスコピー時の視機能障害も大きな問題であるが，これも頚部硬膜外腔圧の上昇に伴い脳脊髄液圧が上昇し，視神経および眼球の栄養血管が圧迫され虚血，出血をきたすことが病因と考えられる．硬膜外腔への薬液注入とエピドラスコピーで生じた視機能障害発症症例12例を解析した文献によると，薬液の投与量は20～120ml(平均59.4ml)であり，その58.3%に網膜出血がみられた．また79.2%の症例で視機能の回復をみたとされている[3]．

Ⅲ　使用薬剤に起因する合併症

エピドラスコピーによる癒着剥離では，硬膜外腔にさまざまな薬剤が投与される．具体的には，造影剤，局所麻酔薬，ステロイドなどである．薬剤に対する合併症で問題となるのは，これらの薬剤に対するアレルギー，アナフィラキシーと，薬剤の血管内，脳脊髄液内投与である．薬剤に対するアレルギーに対しては，術前に問診を行い確認することが重要である．薬剤の血管内，脳脊髄液内投与を予防するためには，カテーテルシャフトでの癒着剥離を愛護的に行うことはもとより，必要に応じて内視鏡所見の確認，造影を行い硬膜外腔投与になっていることを確認するのが重要である．われわれは外来での仙骨硬膜外ブロック後に局所麻酔薬中毒を発症した症例や，エピドラスコピーの適応決定のために行う仙骨硬膜外造影で，血液の逆流がまったくないにもかかわらず硬膜外腔の細い静脈が造影される症例(図2)を数例経験しており，特に局所麻酔薬やステロイドなどの薬物の注入は緩徐に行うべきであると考える．エピドラスコピー施行時の造影剤の偶発的血管内注入については文献的にも報告されている[4]．

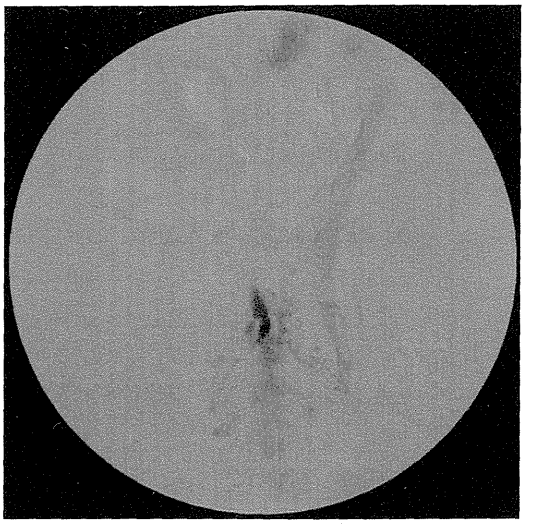

図2　仙骨硬膜外造影(偶発的血管内注入)
仙骨裂孔から21Gのスパイナル針を用いて仙骨硬膜外造影を行った．仙骨硬膜外腔からその周囲の細い静脈(おそらく仙骨硬膜外腔壁の静脈叢)に造影剤が漏れ出している．右側の太い血管は下大静脈である．この症例では穿刺針からの血液の逆流はまったく認められなかった．

以下に各使用薬剤に対する注意点と起こりうる合併症について記載する.

1. 局所麻酔薬

エピドラスコピーで通常使用される局所麻酔薬は,リドカイン,メピバカイン,ロピバカインなどのアミド型が中心であり,エステル型に比べてアレルギー,アナフィラキシーの発症頻度は低いとされる.しかし,発赤,発疹,血圧低下,気管支痙攣を認めた場合はアナフィラキシーを疑い,ステロイド,昇圧剤,輸液などの治療を遅滞なく行う必要がある.

また,血管内に局所麻酔薬が注入されると局所麻酔薬中毒を発症する場合がある.癒着剥離中は患者の様子を注意深く監視し,全身痙攣などが起これば,速やかに気道確保と抗痙攣薬(ジアゼパムなど)の投与を行う必要がある.しかし,発症が急激である場合は脳脊髄液圧亢進による痙攣と区別がつかない場合もありうる.

前述のように,脳脊髄液内に局所麻酔薬が注入されると,くも膜下ブロックとなり,場合によってはブロックが高位に及ぶ場合もある.硬膜外腔投与でも,局所麻酔薬が過量な場合や交感神経ブロック効果が高い場合には,血圧低下などの症状を引き起こすことがあるため,留意する必要がある.

2. 造影剤

エピドラスコピーでの癒着剥離中は,癒着剥離の達成度,髄液内注入の有無,神経根の確認等の目的で造影剤を使用する.使用する造影剤は非イオン性ヨード造影剤(イオヘキソール,イオパミドール,イオトロラン)であり,いわゆるⅠ型アレルギー(アナフィラキシー型)による重篤なショックの発現率は0.04%で低いとされている[5].この場合は,血圧低下などの症状をきたすので速やかにステロイド,昇圧剤,輸液などの治療を行う必要がある.それ以上に注意が必要なのは,非イオン性造影剤では,遅発性の非Ⅰ型アレルギー反応といわれる過敏反応が起こる可能性があることである.これは造影剤使用後2～3日目より出現し,著明な低血圧,頸部・胸部の紅斑,白血球増加,CRP上昇,肝機能障害などがみられる[6].エピドラスコピーは短期入院の場合が多く,施設によっては日帰り手術で行われることもあるので念頭におく必要がある.

Mizunoらは,造影剤の脳脊髄液内注入が原因と考えられる以下のような症例を報告している.76歳男性のFBSS(failed back surgery syndrome)患者にエピドラスコピーによる癒着剥離を施行したところ,術後当日,両下肢筋力低下に続いて,意識混濁,興奮状態,尿失禁を認め,血液データ上CPK,ミオグロビンの上昇がみられた.頭部CTを撮影したところ脳室内が著明に造影されたことから,使用したイオトロランの脳脊髄液内注入による脳症,横紋筋融解症が疑われた.幸い,頭高位と輸液療法で後遺症なく回復したとされている[7].イオトロランは脊髄造影にも使用される造影剤であるが,過量投与になると思わぬ合併症を引き起こす危険性があることを認識する必要がある.

3. ステロイド

ステロイドはその抗炎症作用や細胞膜安定化作用に期待して,エピドラスコピー施行時には頻用されている薬剤である.半減期が36～54時間と比較的長いことからベタメタゾンやデキサメタゾンが使用されることが多い.副作用としては免疫抑制,耐糖能異常,消化管潰瘍などがあるが,単回の使用で問題となることはまずない.投与経路では,ステロイドの硬膜外投与での合併症はほぼ皆無であるが,くも膜下注入ではくも膜炎を生じる可能性があるため注意を要する.

Ⅳ　感染に起因する合併症

エピドラスコピーでは,仙骨下部の皮膚に小切開を施し仙骨裂孔にシースを挿入し,それを介して硬膜外腔にビデオガイドカテーテルを挿入して,硬膜外腔の癒着剥離を行う.また,癒着剥離操作によって硬膜,くも膜に微細な損傷を生じることも少なくない.こうした進入経路から考えると,エピドラス

コピーによって創部，硬膜外腔，髄膜に感染を生じる可能性がある．具体的には，硬膜外膿瘍，細菌性髄膜炎，ウイルス性髄膜炎，創部感染である．現在まで文献的にはこれらの感染に関係する合併症の報告はなく，自験例でも感染例には遭遇していない．しかし，創部は陰部に近く，尿路，肛門の近傍となるため，術後は特に清潔に保つ必要がある．

われわれは感染予防対策として，術中，術後の予防的抗生物質投与，整形外科手術と同様の厳密な術中清潔操作を行っている．また，術後，抜糸までの期間の創部感染予防策として，排泄後のウォシュレットの使用や陰部清潔保持の指導を行っている．

まとめ

エピドラスコピーの合併症・偶発症について原因別に整理し，合併症に関係した自験例や症例報告を交えて，その予防策・対応策を概説した．術中は脳脊髄液圧上昇が原因となる合併症が最も頻度が高く，重篤になる可能性が高いため注意が必要である．また，まれな合併症についても念頭においてエピドラスコピーを施行することが，合併症回避につながり，エピドラスコピーの安全性をより高めることにつながると考えられる．

参考文献

1) 上野博司，細川豊史，山下智充ほか：Epiduroscopy施行時に頭痛を訴えた2症例―頚部硬膜外腔圧と頭痛発症との相関―．日本ペインクリニック学会誌 9：446-450, 2002
2) 浅野真，大岡卓司，小坂義弘：硬膜外腔圧と脳脊髄液圧の関係．麻酔 36：89-93, 1987
3) Gill JB, Heavner JE : Visual impairment following epidural fluid injections and epiduroscopy : a review. Pain Med 6 : 367-374, 2005
4) Heavner JE, Wyatt DE, Bosscher HA : Lumbosacral epiduroscopy complicated by intravascular injection. Anesthesiology 107 : 347-350, 2007
5) Barrett BJ, Parfrey PS, Vavasour HM, et al. : A comparison of nonionic, low-osmolarity radiocontrast agents with ionic, high-osmolarity agents during cardiac catheterization. N Engl J Med 326 : 431-436, 1992
6) 十倉正朗，川崎繁，名嘉山一郎：非イオン性造影剤の使用で重篤な遅発性副作用のみられた2症例．外科 57：864-868, 1995
7) Mizuno J, Gauss T, Suzuki M, et al. : Encephalopathy and rhabdomyolysis induced by iotrolan during epiduroscopy. Can J Anaesth 54 : 49-53, 2007

Complications and Accidental Symptoms in Epiduroscopy

Hiroshi UENO, Keita FUKAZAWA, Akiho HARADA, Toyoshi HOSOKAWA
Department of Anesthesiology, Kyoto Prefectural University of Medicine

Complications in epiduroscopy are classified in the following three major categories : procedural complications, drug-induced cases and infections.

First, cerebrospinal pressure is elevated, because a large quantity of physiologic saline is injected into the epidural space during percutaneous epiduroscopic adhenolysis. Therefore, some complications such as headache, cervicodynia, convulsions and visual impairment have been reported frequently.

Second, allergic and anaphylactic reactions to local anesthetics and radiocontrast agent must be considered. Also, we have to know that such drugs can be occasionally injected into blood or cerebrospinal fluid.

Third, it is important that we do epiduroscopic adhenolysis under sterile conditions and keep the postoperative wound clean to prevent perioperative infection.

To provide an extra margin of safety in epiduroscopy, it is necessary to have full knowledge about the complications and accidental symptoms, and to understand the treatment and prevention methods for them.

Key Words : Epiduroscopy, Complications, Accidental symptoms, Prevention method

The Journal of Japan Society for Clinical Anesthesia Vol.30 No.2, 2010

Journal of Neurochemistry

JOURNAL OF NEUROCHEMISTRY | 2010 | 112 | 521–530 doi: 10.1111/j.1471-4159.2009.06473.x

Parathyroid hormone 2 receptor is a functional marker of nociceptive myelinated fibers responsible for neuropathic pain

Misaki Matsumoto,* Saori Kondo,* Ted B. Usdin† and Hiroshi Ueda*

*Division of Molecular Pharmacology and Neuroscience, Nagasaki University Graduate School of Biomedical Sciences, Nagasaki, Japan

†Section on Fundamental Neuroscience, NIMH, Bethesda, Maryland, USA

Abstract

We have previously demonstrated that parathyroid hormone 2 (PTH2) receptors are expressed in dorsal root ganglion (DRG) neurons and that its endogenous agonist tuberoinfundibular peptide of 39 residues (TIP39) causes nociceptive paw flexor responses after intraplantar administration. Here we found that the PTH2 receptor is selectively localized on myelinated A-, but not unmyelinated C-fibers using immunohistochemical labeling, based on PTH2 receptor expression on antibody N52-positive medium/large-sized DRG neurons, but not on TRPV1, substance P, $P2X_3$ receptor or isolectin B4-binding protein-positive small-sized DRG neurons. Pharmacological studies showed that TIP39-induced nociceptive responses were mediated by activation of G_s and cAMP-dependent protein kinase. We also found that nociceptive responses induced by TIP39- or the cAMP analog 8-bromo-cAMP were significantly greater following partial sciatic nerve injury induced neuropathic pain, without changes in PTH2 receptor expression. Together these data suggest that activation of PTH2 receptors stimulates nociceptive A-fiber through G_s-cAMP-dependent protein kinase signaling, and this pathway has elevated sensitization following nerve injury.

Keywords: cyclic AMP-dependent protein kinase, neuropathic pain, nociception, PTH2 receptor, TIP39.

J. Neurochem. (2010) **112**, 521–530.

The parathyroid hormone 2 (PTH2) receptor, which has ~50% amino acid sequence identity with PTH1 receptor, was identified in 1995 (Usdin *et al.* 1995). The PTH2 receptor is expressed at relatively high levels in several nervous system areas, including parts of the limbic system, several hypothalamic nuclei and the median eminence (Usdin *et al.* 1999a, 2003; Wang *et al.* 2000). It is expressed at very low levels in kidney and bone, where the PTH1 receptor is highly expressed (Urena *et al.* 1993). Interestingly, PTH2 receptors are also expressed in dorsal root ganglion (DRG) neurons as well as the spinal cord dorsal horn, suggesting that PTH2 receptors may play a role in pain regulation (Usdin *et al.* 1999a; Dobolyi *et al.* 2002). Indeed, we found that intraplantar injection of its endogenous agonist tuberoinfundibular peptide of 39 (TIP39) elicited nociceptive flexor responses in mice (Dobolyi *et al.* 2002). In addition, the intrathecal administration of TIP39 potentiated thermal and mechanical responses, as well inducing a nocifensive response (Dobolyi *et al.* 2002). These findings suggest that TIP39 may have pharmacological and physiological effects on nociceptive fibers, but these effects remain to be defined.

Through a series of studies, we have developed several strategies to characterize the *in vivo* signal transduction of specific key molecules involved in pain regulation (Ueda 2006, 2008). One of these strategies is the use of the algogenic-induced paw flexion (APF) test, in which the amplitude of nociceptive flexor responses induced by intraplantar injection (i.pl.) of algogenics is quantitatively

Received July 16, 2009; revised manuscript received September 24, 2009; accepted October 3, 2009.

Address correspondence and reprint requests to Hiroshi Ueda, Division of Molecular Pharmacology and Neuroscience, Nagasaki University Graduate School of Biomedical Sciences, 1-14 Bunkyo-machi, Nagasaki 852-8521, Japan. E-mail: ueda@nagasaki-u.ac.jp

Abbreviations used: 8-Br-cAMP, 8-bromo-cAMP; ABL, algogenic biting and licking; APF, algogenic stimulation-induced paw flexion; AS-ODN, antisense oligodeoxynucleotide; CNQX, 6-cyano-7-nitroquinoxaline-2,3-dione; DRG, dorsal root ganglion; GAPDH, glyceraldehyde-3-phosphate dehydrogenase; i.pl., intraplantar injection; i.t., intrathecal injection; IB4, isolectin B4; MS-ODN, mismatch scramble oligodeoxynucleotide; PKA, cAMP-dependent protein kinase; PTH, parathyroid hormone; TIP39, tuberoinfundibular peptide of 39; TRPV1, transient receptor potential vanilloid 1.

evaluated (Inoue *et al.* 2003b; Ueda 2006). From its careful characterization, the APF test was found to be less stressful and more sensitive than other nociceptive tests. Using this test, the i.pl. administration of test substances can be combined with intrathecal delivery of antisense oligodeoxynucleotides (AS-ODNs) targeting potential effector molecules, such as G proteins (specifically α-subunits) to characterize the *in vivo* signal transduction of pain-producing stimuli. We previously showed study that large amounts of intrathecally administered FITC-labeled AS-ODN accumulate within DRG, while little if any, is detectable in the superficial region of spinal dorsal horn (Ueda 1999). This approach has been used a number of times to inhibit gene expression in DRG (Inoue *et al.* 2003a, 2004; Rashid *et al.* 2004; Matsumoto *et al.* 2007). Neonatal capsaicin-treatment allows responses to be classified as mediated by myelinated A- or unmyelinated C-fibers, as this treatment destroys unmyelinated C-fibers (Hiura and Ishizuka 1989; Rashid *et al.* 2003). We also used pharmacological blockade of nociceptive responses by intrathecal administration of specific antagonists for substance P (NK1 receptor) or glutamate (NMDA or non-NMDA receptors), which are representative spinal pain transmitters. Using these strategies, we have successfully characterized signal transduction and sensory fibers that are involved in nociceptive responses caused by pain-producing stimuli, such as bradykinin, substance P, ATP, prostaglandin I_2 agonist, nociceptin and nocistatin (Inoue *et al.* 1998a, 2003a,c; Matsumoto *et al.* 2006; Ueda 2006).

These strategies led to the finding that the neuropathic pain model with partial injury of the sciatic nerve shows a decrease in C-fiber-mediated responses, whereas significant enhancement in A-fiber-mediated responses (Rashid *et al.* 2003; Inoue *et al.* 2006; Ueda 2006). These findings are supported by a study using biochemical markers, in which C-fiber stimulation-induced spinal neuronal activation was reduced while A-fiber stimulation-induced neuronal activation was up-regulated (Matsumoto *et al.* 2008). Thus, we have proposed a dominant role of A-fibers in neuropathic pain.

In the present study, we first performed an immunohistochemical characterization of the cell population that expresses PTH2 receptors in DRG, and second performed a pharmacological characterization of this receptor's role in acute and chronic pain.

Materials and methods

Animals and neonatal capsaicin-treatment

Male ddY mice and male C57BL/6J mice weighing 20–24 g were used after adaptation to the laboratory conditions: 22 ± 2°C, 55 ± 5% relative humidity and a 12 h light/dark cycle with food and water *ad libitum*. Neonatal capsaicin treatment, which causes degeneration of unmyelinated C-fibers, was performed as described previously (Rashid *et al.* 2003) by subcutaneous (s.c.) injection of 50 mg/kg capsaicin (Nacalai Tesque, Kyoto, Japan) into newborn (P4) pups. Animal procedures were approved by the Nagasaki University Animal Care Committee, and complied with the fundamental guidelines for proper conduct of animal experiments and related activities in academic research institutions under the jurisdiction of the Ministry of Education, Culture, Sports, Science and Technology, Japan.

Neuropathic pain model

Partial ligation of sciatic nerve of mice was performed under pentobarbital (50 mg/kg, i.p.) anesthesia, as described previously (Rashid *et al.* 2003; Inoue *et al.* 2004; Matsumoto *et al.* 2008). Briefly, the common sciatic nerve of the right hind limb was exposed at high thigh level through a small incision and half of the nerve thickness was tightly ligated with a silk suture. Sham surgery was performed similarly, except without touching the sciatic nerve. Most of the experiments in this study were carried out on the 7th day after the sham or nerve injury surgery. At this time point, significant thermal hyperalgesia and mechanical allodynia were observed (Inoue *et al.* 2004).

Drugs

The following drugs were used: Capsaicin (Nacalai Tesque), (+)-5-methyl-10,11-dihydro-5H-dibenzo[a,d]cyclohepten-5,10-imine hydrogen maleate (MK-801), 6-cyano-7-nitroquinoxaline-2,3-dione (CNQX) (Research Biochemicals International, Natick, MA, USA), 8-bromo-cAMP (8-Br-cAMP), H-89 dihydrochloride hydrate (Sigma, St. Louis, MO, USA), pertussis toxin and U-73122 (Funakoshi, Tokyo, Japan), and KT-5720 (Wako, Tokyo, Japan). Mouse TIP39 was synthesized by Midwest Biomolecules (Waterloo, IL, USA). CP-99994 was generously provided by Pfizer Pharmaceuticals (Sandwich, Kent, UK). All drugs except KT-5720 and capsaicin were dissolved in physiological saline. KT-5720 was dissolved in 30% dimethyl sulfoxide, while capsaicin was dissolved in 10% ethanol and 10% Tween 80 in physiological saline.

Oligodeoxynucleotide treatments

The AS-ODN against the PTH2 receptor (5′-ATCCACAAATG-TAGGTGAAA-3′) and its mismatch scrambled oligodeoxynucleotide (MS-ODN; 5′-TACCAACAATTGAGGGTAAA-3′), and the AS-ODN against $G\alpha_s$ (5′-AGTCACCCATTAGTGACGCC-3′), and its MS-ODN (5′-AGCTACCACTATGTGCAGCC-3′) were synthesized by Operon Biotechnologies (Tokyo, Japan). The oligodeoxynucleotides were freshly dissolved in artificial CSF comprised of 125 mM NaCl, 3.8 mM KCl, 2.0 mM $CaCl_2$, 1.0 mM $MgCl_2$, 1.2 mM KH_2PO_4, 26 mM $NaHCO_3$ and 10 mM D-glucose (pH 7.4) and injected intrathecally (i.t.) between the L5 and L6 lumbar space in unanesthetized mice using a 30-gauge needle. The treatment was performed (10 μg/5 μL) on the 1st, 3rd and 5th days, as stated in our previous study (Ueda and Inoue 2000; Matsumoto *et al.* 2007). On the 6th day, the treated mice were assessed in behavioral tests, and tissues were isolated for western blot and immunohistochemical experiments.

Western blot analysis

To confirm the effect of AS-ODN for PTH2 receptor and $G\alpha_s$, sodium dodecyl sulfate–polyacrylamide gel electrophoresis using 12% polyacrylamide gel and immunoblot analysis were performed

as described (Ueda and Inoue 2000). Twenty μg of protein extracted from the L4–6 dorsal root ganglion (DRG) was used. To get equal transfer efficiency, we applied all samples to the same gel and carried out the immunoblot transfer using the same membrane. Visualization of immunoreactive bands was performed by use of an enhanced chemiluminescent substrate for detection of horseradish peroxidase, Super Signaling Substrate (PIERCE, Rockford, IL, USA). The intensities of the immunoreactive bands were analyzed by NIH Image for Macintosh after scanning exposed films.

Nociception tests

The algogenic-induced paw flexion test

Experiments were performed as described previously (Dobolyi *et al.* 2002; Inoue *et al.* 2003b; Ueda 2006). Briefly, mice were held in a cloth sling with their four limbs hanging free through holes. The sling was suspended from a metal bar. All limbs were tied with strings, and three were fixed to the floor, while the 4th was connected to an isotonic transducer and recorder. A polyethylene cannula (0.61 mm in outer diameter) filled with drug solution was connected to microsyringe and then carefully inserted into the undersurface of the right hind paw. In the dose-response experiments and the experiment with AS-ODN, we used the biggest response among spontaneous and non-specific flexor responses occurring immediately after cannulation as the maximal reflex, as the intensity of flexor responses differs from mouse to mouse. In these experiments, TIP39 was administered i.pl. through the cannula at 5-min intervals. Averages of two responses to each TIP39 dose were evaluated. In the experiment with inhibitors, TIP39 was administered 10 and 5 min (control TIP39-response) prior to and 5, 10, 20 and 30 min after the inhibitor (or vehicle)-injection. The results were expressed as percent of control response, using the following equation: [TIP39-response (mm) after the inhibitor administration/the average of two control TIP39-responses (mm)] × 100 (%).

The algogenic-induced biting and licking test

Experiments were performed as described previously (Inoue *et al.* 2003b). Mice were placed individually in plastic cages for 1 h to adapt to the environment. Algogenics in a volume of 20 μL were injected into the right hind paw of mice (i.pl.) using a 30-gauge needle fitted to 50 μL volume Hamilton microsyringe. In the experiments using antagonists, 2 μL antagonist was injected (i.pl) 20 min prior to the algogen in a 20 μL volume. Each mouse was immediately put back in its cage and the time spent biting and licking the injected paw was measured for a period of 10 min after injection. Saline was injected as a control.

Immunohistochemistry

Anesthetized mice were transcardially perfused with phosphate-buffered saline, followed by cold 4% paraformaldehyde solution. The L4–6 DRG were isolated, post-fixed for 3 h, and cryoprotected overnight in 25% sucrose solution. The tissues were fast-frozen in cryo-embedding compound on a mixture of ethanol and dry ice and stored at −80°C until use. DRG were cut on a cryostat at a thickness of 10 μm, thaw-mounted on silane-coated glass slides, and air-dried overnight at 25°C. Sections were incubated with blocking buffer containing 2% bovine serum albumin in PBST (0.1% Triton X-100 in phosphate-buffered saline) and subsequently reacted overnight at 4°C with rabbit antibody against PTH2 receptor (1 : 3000) in the blocking buffer (Usdin *et al.* 1999a,b). After thorough washing, the sections were incubated with secondary antibody, Alexa Fluor 488-conjugated anti-rabbit IgG (1 : 500; Invitrogen, Carlsbad, CA, USA), for 120 min at 25°C, and coverslipped with PermaFluor (Thermo Shandon, Pittsburgh, PA, USA). For double immunolabeling, we used the following antibodies: a mouse monoclonal antibody against N52 clone of Neurofilament 200, a marker of myelinated fibers (anti-N52; 1 : 30 000; Sigma); a goat polyclonal antibody against transient receptor potential vanilloid 1 (TRPV1); a rabbit polyclonal antibody against Substance P; a guinea pig polyclonal antibody against $P2X_3$ (Chemicon, Temecula, CA, USA); FITC-conjugated isolectin B4 (IB4; 10 μg/mL; Sigma); Alexa Fluor 488-conjugated anti-rabbit IgG; Alexa Fluor 594-conjugated anti-rabbit IgG; Alexa Fluor 488-conjugated anti-mouse IgG; Alexa Fluor 488-conjugated anti-goat IgG; Alexa Fluor 488-conjugated anti-guinia pig IgG (1 : 300; Molecular probes). Sections were examined under a BX-50 fluorescence microscopy (Olympus, Tokyo, Japan) or a BZ-8000 fluorescence microscopy (Keyence, Tokyo, Japan). Digital images were acquired with either ×10 objective or ×20 objective, and neurons with visible nuclei were evaluated. The diameters of DRG neurons were measured and calculated from a line drawn by the operator using AxioVision 3.1 software (Carl Zeiss, Oberkochen, Germany) and BZ-analyzer software (Keyence), respectively.

Quantitative real-time PCR

The L4–6 DRGs were isolated and RNA was purified using TRIzol (Invitrogen, Carlsbad, CA, USA). Total RNA (1 μg) was used for cDNA synthesis with Superscript II reverse transcriptase and random hexamer primers (Invitrogen). Real-time quantitative PCR (RT-PCR) was performed using an ABI Prism 7000 Sequence Detection system (Applied Biosystems, Tokyo, Japan), using qPCR MasterMix Plus for SYBR® Green I (Eurogentec, Seraing, Belgium) containing dNTPs (+dUTP), Hot Goldstar DNA polymerase, and Urasil-*N* Glycosilase, according to the manufactures instructions. The cycling conditions for all primers were the following: 10 min at 95°C to activate the Hot Goldstar DNA polymerase, followed by 50 cycles consisting of two steps, 15 s at 95°C (denaturation) and 1 min at 60°C (annealing-extension). The PTH2 receptor mRNA levels were evaluated by comparison to glyceraldehyde-3-phosphate dehydrogenase (GAPDH). Primer sequences were as follows; PTH2 receptor, (F)5′-GATGGCTGATTCTCAGTAGCTGTCT-3′ and (R)5′-CACACTGCATTTTAGCCTTCATAAC-3′ corresponding to the mouse PTH2 receptor gene (NCBI accession number; AK045576), GAPDH, (F)5′-TATGACTCCACTCACGGCAAAT-3′ and (R)5′-GGGTCTCGCTCCTGGAAGAT-3′ corresponding to the mouse GAPDH (NCBI accession number; NM_001001303). In all cases, the validity of amplification was confirmed by the presence of a single peak in the melting temperature analysis and linear amplification against the PCR cycle number.

Statistical analysis

Data were analyzed using an unpaired Student's *t*-test. Experiments with multiple groups were analyzed using one-way ANOVA with

Tukey-Kramer multiple comparison *post-hoc* analysis. The criterion of significance was set at $p < 0.05$. All results are expressed as mean ± SEM from four to six separate mice.

Results

The PTH2 receptor is expressed by medium/large-sized myelinated DRG neurons

Parathyroid hormone 2 receptor immunoreactive neurons in dorsal root ganglia (DRG) appeared larger than neurons expressing several C-fiber marker proteins, including TRPV1, substance P, the $P2X_3$ receptor and IB4-binding protein (Fig. 1a). There appeared to be no neurons that co-expressed the PTH2 receptor and any of the C-fiber marker proteins (Fig. 1b). Instead, approximately 70% of the neurons expressing the PTH2 receptor were also positive for N52, a monoclonal antibody against neurofilament 200, which is a representative molecular marker for myelinated A-fibers (Fig. 1a and b). A size distribution study demonstrated that PTH2 receptor labeling was mostly present on medium/large-sized DRG neurons (> 24 μm) that largely overlapped the size distribution of N52-immunoreactive cells. This size distribution was clearly distinguishable from the distribution of TRPV1-immunoreactivitity, which was present on the small-sized DRG neurons (< 24 μm) (Fig. 1c). However, it should be noted that the N52-positive population included larger diameter neurons than the PTH2 receptor-positive population, and there were a few PTH2 receptor-positive cells that were smaller than N52-positive cells.

PTH2 receptor expression in DRG neurons is insensitive to neonatal capsaicin-treatment

When neonatal mice (postnatal day 4) were pre-treated with 50 mg/kg (s.c.) capsaicin, TRPV1-positive neurons were substantially lost in DRG, while PTH2 receptor-positive ones were not affected (Fig. 2a). In a quantitative analysis, the population of TRPV1-positive neurons was significantly reduced, from 24% to 8%, by the neonatal capsaicin-treatment, while that of PTH2 receptor-positive neurons was slightly but not significantly increased by the capsaicin-treatment (Fig. 2b). This increase in the ratio of PTH2 receptor-positive neurons to total number of neurons could be attributed to the specific loss of the C-fibers induced by the neonatal capsaicin-treatment (Hiura 2000; Nakagawa and Hiura 2006).

TIP39 stimulates NMDA receptor-mediated glutamatergic pain transmission via A-fibers

As previously reported (Dobolyi *et al.* 2002), intraplantar injection of TIP39, the endogenous agonist for the PTH2 receptor (Usdin *et al.* 1999a), dose-dependently caused nociceptive flexor responses in the range between 10 fmol and 100 pmol in the APF test in ddY mice (data not shown). The flexor responses elicited by TIP39 (100 pmol, i.pl.) were significantly reduced by i.t. pre-treatment with an AS-ODN against the PTH2 receptor, but not with a scrambled MS-ODN, as shown in Fig. 3(a). Western blot analysis of DRG preparations showed that AS-ODN markedly reduced the level of PTH2 receptor immunoreactivity, while MS-ODN did not (Fig. 3a-i). TIP39 (100 pmol, i.pl.)-induced nociception in the APF test was not affected by neonatal capsaicin-

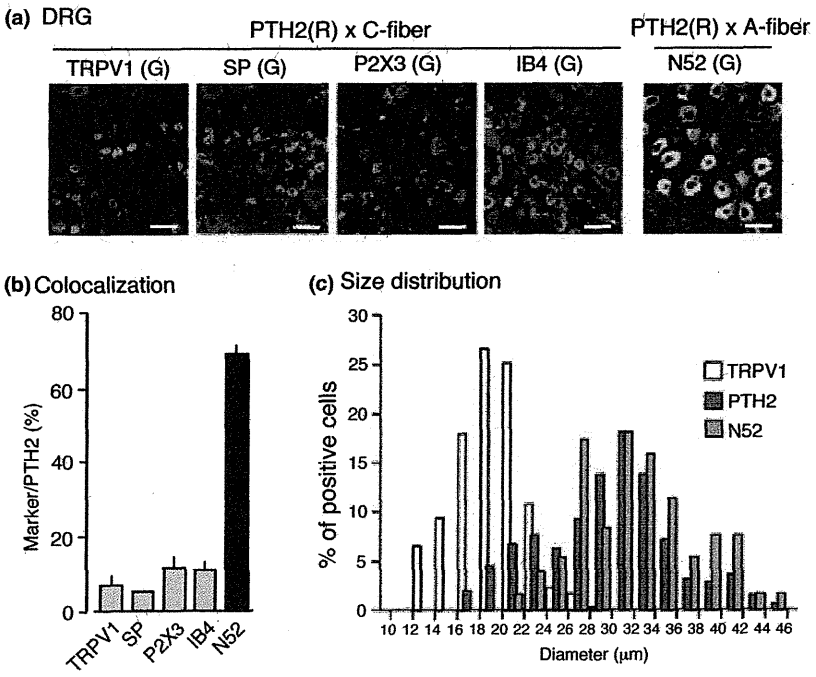

Fig. 1 PTH2 receptor expression in medium/large-sized myelinated DRG neurons. (a) Representative pictures of PTH2 receptor-immunoreactivity (red: R) and other markers (green: G) in the DRG. (b) Quantification of the colocalization of PTH2 receptor labeling with various markers in the DRG. Vertical axis indicates the percentage of PTH2-immunoreactive cells with colocalization of the marker. (c) The size distribution of DRG neurons labeled with TRPV1, PTH2 receptor or N52 antibodies. Vertical axis indicates the percentage of the total number of immunoreactive cells labeled for each marker. Only neurons with clearly visible nuclei were counted. SP, substance P; IB4, IB4-binding protein; N52, N52 clone for neurofilament 200. Scale bar = 50 μm. Cells from two or three DRG sections from three separate ddY mice were counted. Data represent the means ± SEM.

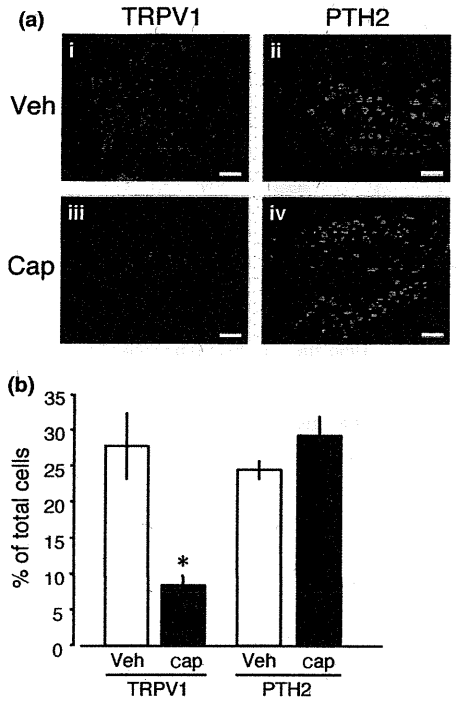

Fig. 2 PTH2 receptor expression in DRG neurons is insensitive to neonatal capsaicin-treatment. (a) Representative pictures of TRPV1-immunoreactivity (red) and of PTH2 receptor-immunoreactivity (green) in the DRG of neonatal capsaicin-treated (Cap) or vehicle-treated (Veh) mice. (b) Results of quantification of TRPV1-positive or PTH2 receptors-positive cells in the DRG. Vertical axis indicates the percentage of positive cells as a portion of the total number of DRG cells. Scale bar = 100 μm. Cells on two or three DRG sections from three separate ddY mice per condition were counted. $^*p < 0.05$ vs. vehicle treatments (Veh). Data represent the means ± SEM.

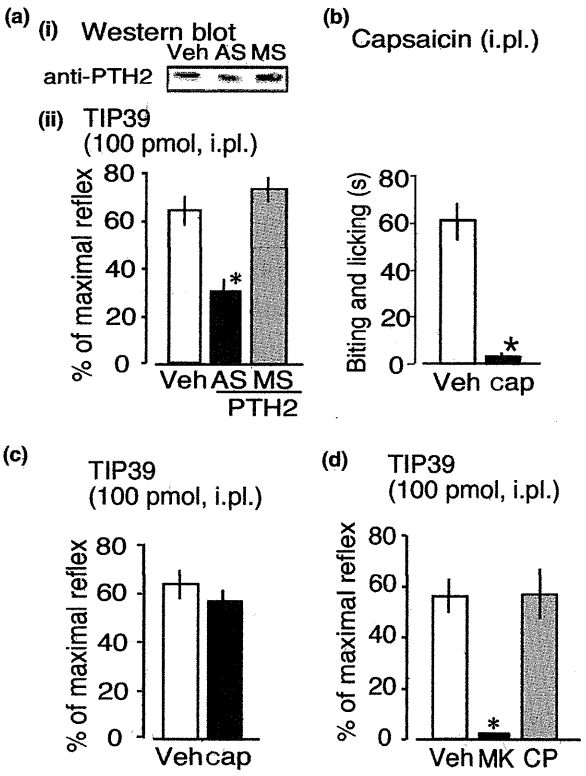

Fig. 3 TIP39 stimulates A-fibers to cause glutamate-NMDA receptor pain transmission. (a) Effects of AS-ODN (AS) or MS-ODN (MS) against the PTH2 receptor. (i) The reduction of PTH2 receptor protein in L4–6 DRGs by its AS-ODN. Photograph shows a representative western blot. (ii) Effect of AS-ODN on TIP39 (100 pmol, i.pl.)-induced flexor responses in the APF test. The response was normalized to the maximal reflex, as the intensity of flexor responses differs from mouse to mouse (see Materials and methods). (b) Block of acute capsaicin (0.8 μg, i.pl.)-induced nociceptive biting and licking responses after 10 min in neonatal capsaicin-treated mice. (c) Lack of effect of neonatal capsaicin-treatment on TIP39 (100 pmol, i.pl.)-induced responses in the APF test. (d) Block of TIP39 (100 pmol, i.pl.)-induced nociception by the intrathecal pre-treatment with MK-801 (3 nmol; MK) but not with CP-99994 (3 nmol; CP). Vehicle or drugs were intrathecally administered 20 min prior to TIP39 injection. $^*p < 0.05$ vs. vehicle treatments (Veh). Data represent the means ± SEM from experiments using 4–6 ddY mice.

pretreatment, which abolished the acute capsaicin (i.pl.)-induced nocisponsive biting and licking behaviors (Fig. 3b and c).

When MK-801 (3 mol), a non-competitive NMDA receptor antagonist, was given intrathecally 20 min prior to TIP39 (100 pmol, i.pl.), TIP39-induced flexor responses were completely abolished (Fig. 3d). However, as shown in Fig. 3(d), the TIP39-induced responses were not affected by the NK1 receptor antagonist CP-99994 (3 mol, i.t.), which significantly blocks bradykinin (i.pl.)- or substance P (i.pl.)-induced flexor responses (Inoue *et al.* 2003c).

Similarly, MK-801 (3 nmol, i.t.) but not CP-99994 (3 nmol, i.t.) attenuated the TIP39 (100 fmol, i.t.)-induced nociceptive behaviors, such as reciprocal hindlimb scratching, and caudally directed scratching, biting, and licking during 20 min after TIP39 administration (Fig. S1). On the other hand, CNQX (3 nmol, i.t.), an α-amino-3-hydroxy-5-methylisoxazole-4-propionate/kainate receptor antagonist, failed to inhibit the TIP39-induced scratching, biting, and licking responses (Fig. S1).

TIP39 nociceptor signaling is mediated through G_s and PKA

The pre-treatment with AS-ODN against G protein subunit, $G\alpha_s$, markedly reduced the $G\alpha_s$ levels in the DRG (Fig. 4a-i). TIP39 (100 pmol, i.pl.)-induced flexor responses were significantly reduced by the pre-treatment with AS-ODN against $G\alpha_s$, but not by its MS-ODN, as shown in Fig. 4(a). Repeated challenges with TIP39 (100 pmol, i.pl.) at intervals of 5–10 min caused constant responses for at least 30 min (Fig. 4b), suggesting that these repeated TIP39 challenges did not cause desensitization of the PTH2 receptor. When KT-5720, a specific cAMP-dependent protein kinase (PKA) inhibitor, was given (3 nmol, i.pl.) (Inoue *et al.* 2003a) after

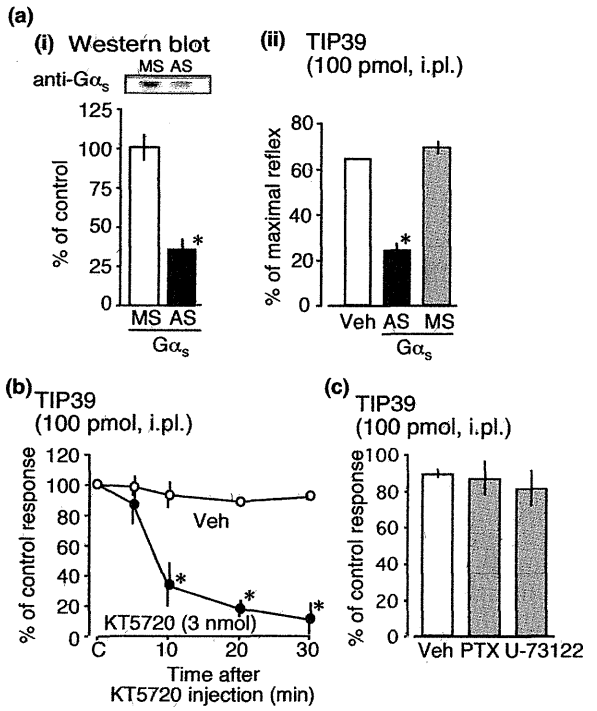

Fig. 4 *In vivo* signal transduction of TIP-39-induced nociceptive responses. (a) Effects of AS-ODN (AS) or MS-ODN (MS) against $G\alpha_s$-subunit. (i) The reduction of $G\alpha_s$-subunit protein in L4–6 DRGs by its AS-ODN. Photograph shows a representative western blot. (ii) Effect of AS-ODN on TIP39 (100 pmol, i.p.l.)-induced flexor responses in the APF test. (b) The time-dependent blockade of TIP39 (100 pmol, i.p.l.)-induced flexor responses by a PKA inhibitor KT-5720 (3 nmol, i.p.l.). In this experiment, TIP39 was given at 10 and 5 min (the average is indicated as the control response; C) prior to and 5, 10, 20 and 30 min after the inhibitor (or vehicle)-injection. The results are expressed as percent of control response. (c) Lack of effect of pertussis toxin (PTX) and phospholipase C inhibitor on TIP39 (100 pmol, i.p.l.)-induced nociception. PTX (10 ng; i.p.l.) or U-73122 (10 pmol; i.p.l.) was given 30 min prior to TIP39 injection. $^*p < 0.05$ vs. vehicle treatments (Veh). Data represent the means ± SEM from experiments using 4–6 ddY mice.

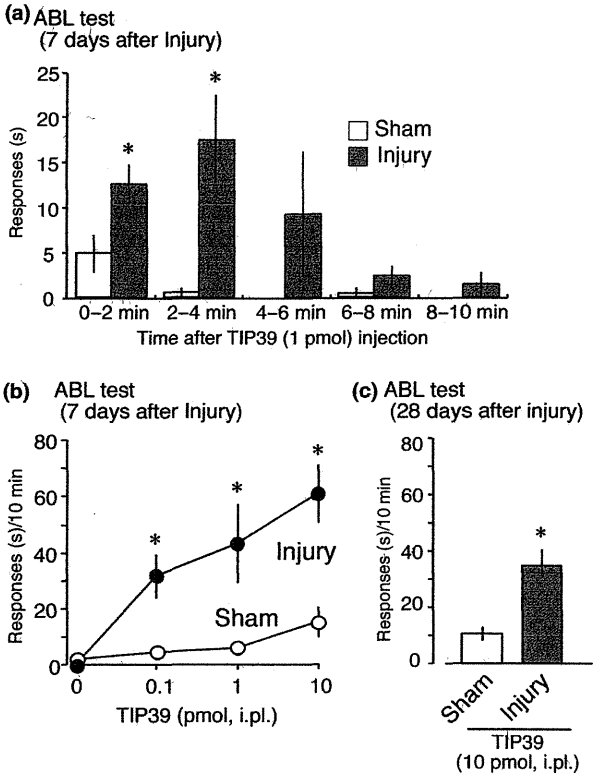

Fig. 5 Hypersensitization of responses to TIP39 in nerve injured mice. (a) Time course of effects of TIP39 (1 pmol, i.p.l.)-induced nociceptive biting and licking responses in nerve-injured or sham-operated mice in the ABL test. The experiment was carried out on the 7th day after surgery. (b) Dose-response for nociceptive biting and licking responses to TIP39 (i.p.l.) in nerve-injured mice (7th day after surgery) in the ABL test. (c) Elevated nociceptive biting and licking responses to TIP39 (10 pmol, i.p.l.) in nerve-injured mice (28 days after surgery) in the ABL test. $^*p < 0.05$ vs. sham. Data represent the means ± SEM from experiments using 4–6 C57BL/6J mice.

the confirmation of control responses to TIP39, subsequent TIP39 responses were inhibited as early as 10 min after the inhibitor infusion (Fig. 4b), suggesting that the activation of the PTH2 receptor, G_s and PKA is required for TIP39-mediated nociception. In contrast, TIP39 responses were not affected by pertussis toxin (10 ng, i.p.l.) or by U-73122 (3 pmol, i.p.l.), which block receptor-$G_{i/o}$ coupling or a phospholipase C signaling, respectively (Inoue *et al.* 1998b) (Fig. 4c).

Nerve injured mice become hypersensitive to TIP39 without a change in PTH2 receptor expression

Tuberoinfundibular peptide of 39-induced nociceptive responses were analyzed in the nerve injury-induced neuropathic pain model using C57BL/6J mice. In this experiment, mice were injected with vehicle or TIP39, returned to their cage, and algogenic biting and licking (ABL) behaviors quantitated. In the absence of TIP39 (see dose '0' in Fig. 5b), no significant ABL response was observed in sham-operated or nerve-injured mice. As shown in Fig. 5(a), characteristic ABL responses to TIP39 (1 pmol, i.p.l.) were observed between 2 and 5 min in injured mice, and not in sham-operated ones, although transient responses within 1 min were observed in both groups. The TIP39-induced nociceptive responses continued for 10 min after the injection in injured mice and were dose-dependent in the range between 0.1 and 10 pmol (Fig. 5b). However, no substantial responses were observed in sham-operated mice. When the ABL test was carried out 28 days after the injury, the injury-specific TIP39 (10 nmol)-responses were still observed, while the level (35.2 s) was slightly lower than

that (60.7 s) at 7 days (Fig. 5c). Similar enhanced TIP39-induced responses were also observed in ddY mice (Fig. S2).

Quantitative real-time PCR indicated no change in the level of PTH2 receptor mRNA in DRG for up to 7 days following nerve injury, as compared to GAPDH (Fig. 6a). The lack of change of PTH2 receptor level in the DRG following nerve injury was also observed when the PTH2 receptor level was evaluated by immunohistochemistry (Fig. 6b). In addition, the nerve injury did not cause substantial change in the size distribution of PTH2-positive neurons (data not shown).

When 8-bromo-cAMP (8-Br-cAMP), a stable and cell permeable analog of cAMP was given intraplantarly, a characteristic enhancement of ABL behaviors was observed following nerve injury (Fig. 6c). Both TIP39 (10 pmol) and 8-Br-cAMP (10 nmol)-induced hypersensitized ABL responses in nerve-injured mice were significantly attenuated by the PKA inhibitor H-89 (10 nmol), which was given intraplantarly 20 min prior to the test drug administration (Fig. 6d).

Finally, we examined the co-expression of the PTH2 receptor and TRPV1 in the DRG following nerve injury, as TRPV1 is a representative target for PKA (Lopshire and Nicol 1998; Bhave *et al.* 2002), and it is newly expressed in myelinated A-fibers after the nerve injury (Rashid *et al.* 2003). TRPV1 is dramatically up-regulated 7 days after nerve injury and partially co-expressed with PTH2 receptor (Fig. 6e). On the other hand, substantially no co-expression was observed in the DRG of sham-operated mice.

Discussion

In the present study, PTH2 receptor-immunoreactivity was observed in medium/large-sized DRG neurons, and found to

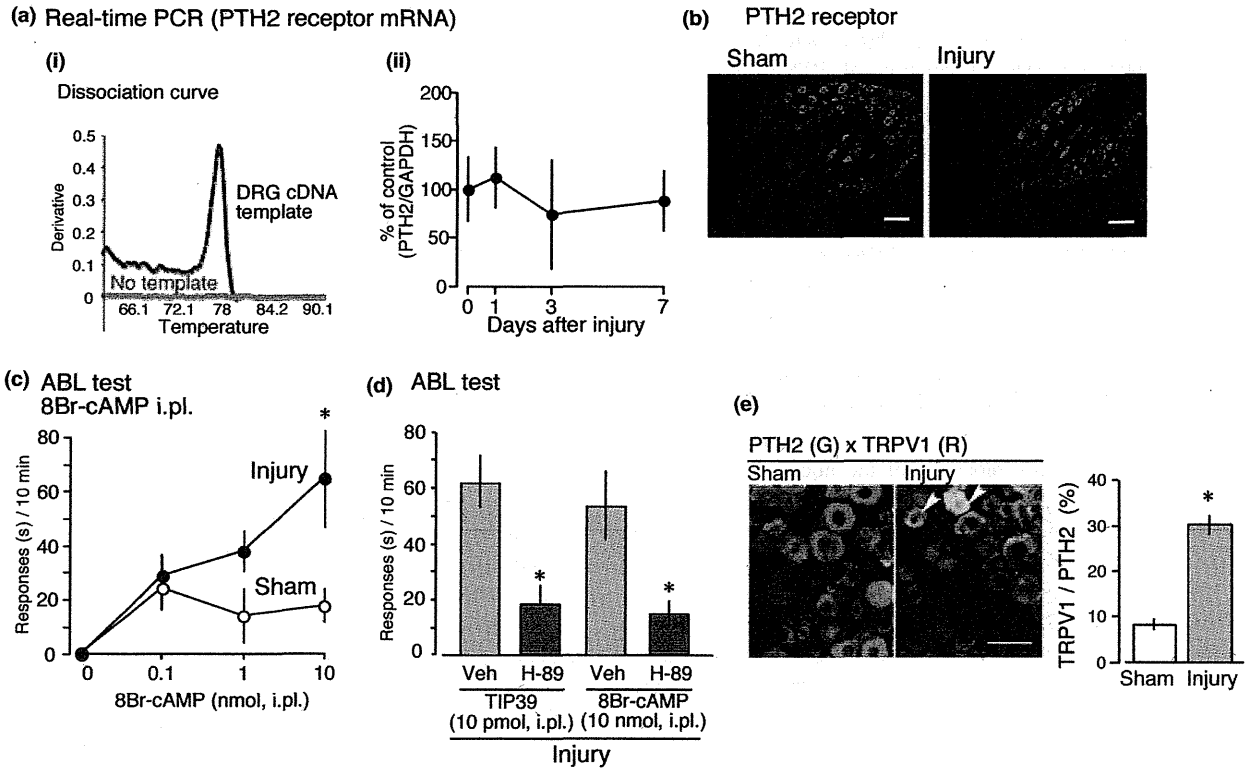

Fig. 6 Lack of PTH2 receptor change and increased sensitivity of a PKA pathway following nerve injury. (a) Lack of change in the PTH2 receptor mRNA level in the L4–6 DRG after nerve injury. (i) Melting curve for the PTH2 receptor real-time PCR reaction. (ii) PTH2 mRNA level normalized to GAPDH mRNA. (b) Lack of change in the PTH2 receptor-immunoreactivity in DRG after nerve injury. The experiment was carried out on the 7th day after the sham or nerve injury surgery. Scale bar = 100 μm. (c) Elevated nociceptive biting and licking responses to 8Br-cAMP (i.pl.) in nerve-injured mice (the 7th day after surgery in the ABL test. (d) Block of TIP39 (10 pmol, i.pl.)-induced hypersensitization and of 8Br-cAMP (10 nmol, i.pl.)-induced hypersensitization in nerve-injured mice (7th day after surgery) by a PKA inhibitor H-89 (10 nmol, i.pl.) in the ABL test. Vehicle (Veh) or H-89 was given 20 min prior to algogenic injection. (e) Representative pictures of PTH2 receptor-immunoreactivity (green: G) and TRPV1 (red: R) in the DRG of sham-operated or nerve-injured mice (7th day after surgery). Quantification of the colocalization was shown in the right. Vertical axis indicates the percentage of PTH2-immunoreactive cells with TRPV1-immunoreactivity. Scale bar = 50 μm. *$p < 0.05$ vs. vehicle treatments (Veh) or sham. Data represent the means ± SEM from experiments using 4–6 C57BL/6J mice.

be substantially co-localized with the myelinated A-fiber marker N52, but not with C-fiber markers. Consistently, the intraplantar injection of TIP39, a potent endogenous agonist of the PTH2 receptor induced nociceptive flexor response through capsaicin-insensitive glutamatergic A-fibers. These results suggest that the PTH2 receptor could be a novel neurochemical marker for nociceptive A-fibers. Many neurochemical markers have been identified for C-fibers, including TRPV1, substance P, calcitonin gene-related peptide, $P2X_3$ receptors, IB4-binding protein, voltage-gated sodium channel $Na_v1.8$, and $Na_v1.9$ (Dib-Hajj *et al.* 1998; Snider and McMahon 1998; Tate *et al.* 1998; Ueda 2006). These molecules are useful not only as pharmacological targets to evaluate or modify C-fiber function (Ueda 2006), but also as genetic targets to specifically label or ablate C-fibers (Braz *et al.* 2005; Abrahamsen *et al.* 2008). On the other hand, fewer neurochemical markers have been identified in A-fibers. The best known marker is neurofilament 200 (N52 or RT97), which is expressed in both Aδ-fibers and Aα/β-fibers (Lawson and Waddell 1991). Using this marker, we found that the size distribution of PTH2-positive DRG neurons overlapped significantly with the distribution of N52-positive cells, but was somewhat smaller on average. This suggests that PTH2 receptor might be expressed in smaller sized A-fibers or Aδ-like-fibers, in view of the fact that there is a positive co-relationship between the conduction velocity and the soma size of DRG neurons (Lawson and Waddell 1991). In addition, TIP39-induced nociceptive responses share the similar pharmacological characteristics in terms of spinal neurotransmission with those by Aδ-fiber stimulation using the Neurometer® method (Matsumoto *et al.* 2008). Both responses were sensitive to MK-801, but not to CP-99994 or CNQX (Matsumoto *et al.* 2006, 2008). The lack of CNQX blockade of the nociceptive responses induced by peripherally applied chemicals was consistent with our previous reports (Inoue *et al.* 2003c; Matsumoto *et al.* 2006, 2008), though α-amino-3-hydroxy-5-methylisoxazole-4-propionate receptor-mediated action is known to precede the NMDA receptor-mediated one. Although details remain to be determined, the lack of CNQX blockade may be explained by recent studies in which the ephrinB-EphB signaling closely related to the NMDA receptor-mediated spinal neurotransmission (Liu *et al.* 2009), facilitates the glutamate-induced NMDA receptor activation in the presence of CNQX (Takasu *et al.* 2002). Although further characterization of A-fibers (Aδ vs. Aβ) requires electrophysiological studies, it is interesting to speculate that the PTH2 receptor might be a functional marker for nociceptive A(δ) fibers. There are reports that other functional molecules, such as $Na_v1.1$, $Na_v1.6$ (Fukuoka *et al.* 2008), $K_v1.1$, $K_v1.2$ (Rasband *et al.* 2001) and TRPV2 (Caterina *et al.* 1999; Lewinter *et al.* 2004) are also expressed by medium/large-sized DRG neurons, though little pharmacological information is available how these molecules are functionally assigned to Aδ-fibers.

It is interesting to discuss the potential source of endogenous TIP39. We have reported that fine scattered TIP39-containing fibers were observed in the lateral funiculus adjacent to the gray matter, an area that contains both descending and primary afferent fibers, and TIP39 mRNA was found in the DRG, but not in the hindpaw or spinal cord (Dobolyi *et al.* 2002). These findings suggest that the source of TIP39 for primary afferent PTH2 receptors seems to be from DRG primary afferent neurons. However, as TIP39-knock out mice showed normal nociception in the mechanical and the thermal test (Fegley *et al.* 2008), endogenous TIP39 is unlikely involved in pain sensation. Thus, primary afferent PTH2 receptors may be the pharmacological target for TIP39, but unlikely have significant physiological roles in pain regulation.

The present study demonstrated that TIP39-induced nociceptive responses in naïve mice are mediated by activation of G_s and PKA, being consistent to the findings with COS-7 cells expressing the PTH2 receptor (Wang *et al.* 2000; Hoare and Usdin 2001). As it is known that G_s-PKA activation has an important role in nociceptor sensitization (Hucho and Levine 2007), the administration of TIP39 may also cause robust sensitization toward physical stimuli, as seen in the report that i.pl. injection of 8-Br-cAMP or forskolin (an activater of adenylate cyclase) in naïve rat produced significant mechanical hyperalgesia (Dina *et al.* 2005).

It should be noted that the nociceptive responses mediated through PTH2 receptors were significantly enhanced in nerve injury-induced neuropathic pain. In the present study, we adopted the ABL test, in which mice are allowed to bite and lick their paw freely to alleviate increased hyperalgesia following injury. The hyperalgesia is unlikely to result from quantitative change in PTH2 receptor expression, as there were no significant changes in the PTH2 receptor protein and gene expression in DRG. Instead the cause seems to be related to post-PTH2 receptor mechanisms, which may include the hypersensitization at the level of primary afferents (Ueda 2006; Hucho and Levine 2007) and spinal neurons (Ji *et al.* 2003). The involvement of post-PTH2 receptor mechanisms was confirmed by the finding that nociceptive behaviors induced by 8-Br-cAMP (i.pl.) was significantly enhanced in nerve-injured mice, possibly through mimicking post-PTH2 receptor signaling. Indeed, the pre-treatment with H-89, a PKA inhibitor, specifically blocked the hyperalgesia to TIP39 or to 8-Br-cAMP in nerve-injured mice. Thus, unidentified mechanisms at the level of PKA activation, or further downstream, seem to underlie the hypersensitivity of PTH2 receptor-expressing A-fibers in neuropathic pain.

One of the targets for PKA would be TRPV1, whose expression occurs in A-fibers following the partial ligation of sciatic nerve of mice, though it is predominantly expressed in C-fibers of naïve mice (Rashid *et al.* 2003). In the present study, we found that co-expression of TRPV1 and PTH2 was significantly increased in the DRG neurons following nerve

injury, which strongly suggests functional interaction in terms of nociceptor sensitization. There are a number of reports that PKA activation causes neuronal hyper-excitability by increasing TRPV1 currents (Lopshire and Nicol 1998; Bhave *et al.* 2002). Other possible targets involved in PKA-mediated A-fiber activation would be voltage-dependent $Na_v1.3$ and calcium channel $\alpha_2\delta$-1 subunit in A-fibers, which are up-regulated by nerve injury (Kim *et al.* 2001; Hains *et al.* 2004). Thus, these mechanisms seem to facilitate generation of action potentials in nociceptive A-fibers, causing hyperalgesic nociceptive response in neuropathic pain. This speculation may be supported by a previous study in which local delivery of a PKA inhibitor to DRG suppressed neuropathic thermal hyperalgesia (Song *et al.* 2006).

In conclusion, we provide evidence that PTH2 receptor-expressing sensory neurons are nociceptive glutamatergic A(δ)-fibers, and that TIP39 as the endogenous ligand of PTH2 receptor is a novel tool to activate this type of nociceptive fiber, and to examine its role in neuropathic hyperalgesia followed by nerve injury. Thus, the PTH2 receptor may be a valuable neurochemical marker that will facilitate investigation of nociceptive A-fibers involved in neuropathic pain.

Acknowledgements

We thank Makoto Inoue for his kind discussion on experimental design. The research described in this article was supported by MEXT KAKENHI-S to H.U. (17109015) and MEXT KAKENHI-C to M.M. (21600007), and Health Labour Sciences Research Grant "Third Term Comprehensive Control Research for Cancer" (398-49) from the Ministry of Health, Labor and Welfare of Japan to H.U. T. U. was supported by the Intramural Program of the National Institute of Mental Health, NIH, USA.

Supporting Information

Additional Supporting Information may be found in the online version of this article:

Figure S1. TIP39 stimulates glutamate-NMDA receptor pain transmission.

Figure S2. Hypersensitization of responses to TIP39 in nerve injured ddY mice.

As a service to our authors and readers, this journal provides supporting information supplied by the authors. Such materials are peer-reviewed and may be re-organized for online delivery, but are not copy-edited or typeset. Technical support issues arising from supporting information (other than missing files) should be addressed to the authors.

References

Abrahamsen B., Zhao J., Asante C. O., Cendan C. M., Marsh S., Martinez-Barbera J. P., Nassar M. A., Dickenson A. H. and Wood J. N. (2008) The cell and molecular basis of mechanical, cold, and inflammatory pain. *Science* **321**, 702–705.

Bhave G., Zhu W., Wang H., Brasier D. J., Oxford G. S. and Gereau R. W. (2002) cAMP-dependent protein kinase regulates desensitization of the capsaicin receptor (VR1) by direct phosphorylation. *Neuron* **35**, 721–731.

Braz J. M., Nassar M. A., Wood J. N. and Basbaum A. I. (2005) Parallel "pain" pathways arise from subpopulations of primary afferent nociceptor. *Neuron* **47**, 787–793.

Caterina M. J., Rosen T. A., Tominaga M., Brake A. J. and Julius D. (1999) A capsaicin-receptor homologue with a high threshold for noxious heat. *Nature* **398**, 436–441.

Dib-Hajj S. D., Tyrrell L., Black J. A. and Waxman S. G. (1998) NaN, a novel voltage-gated Na channel, is expressed preferentially in peripheral sensory neurons and down-regulated after axotomy. *Proc. Natl Acad. Sci. USA* **95**, 8963–8968.

Dina O. A., Hucho T., Yeh J., Malik-Hall M., Reichling D. B. and Levine J. D. (2005) Primary afferent second messenger cascades interact with specific integrin subunits in producing inflammatory hyperalgesia. *Pain* **115**, 191–203.

Dobolyi A., Ueda H., Uchida H., Palkovits M. and Usdin T. B. (2002) Anatomical and physiological evidence for involvement of tuberoinfundibular peptide of 39 residues in nociception. *Proc. Natl Acad. Sci. USA* **99**, 1651–1656.

Fegley D. B., Holmes A., Riordan T. *et al.* (2008) Increased fear- and stress-related anxiety-like behavior in mice lacking tuberoinfundibular peptide of 39 residues. *Genes Brain Behav.* **7**, 933–942.

Fukuoka T., Kobayashi K., Yamanaka H., Obata K., Dai Y. and Noguchi K. (2008) Comparative study of the distribution of the alpha-subunits of voltage-gated sodium channels in normal and axotomized rat dorsal root ganglion neurons. *J. Comp. Neurol.* **510**, 188–206.

Hains B. C., Saab C. Y., Klein J. P., Craner M. J. and Waxman S. G. (2004) Altered sodium channel expression in second-order spinal sensory neurons contributes to pain after peripheral nerve injury. *J. Neurosci.* **24**, 4832–4839.

Hiura A. (2000) Neuroanatomical effects of capsaicin on the primary afferent neurons. *Arch. Histol. Cytol.* **63**, 199–215.

Hiura A. and Ishizuka H. (1989) Changes in features of degenerating primary sensory neurons with time after capsaicin treatment. *Acta Neuropathol. (Berl)* **78**, 35–46.

Hoare S. R. and Usdin T. B. (2001) Molecular mechanisms of ligand recognition by parathyroid hormone 1 (PTH1) and PTH2 receptors. *Curr. Pharm. Des.* **7**, 689–713.

Hucho T. and Levine J. D. (2007) Signaling pathways in sensitization: toward a nociceptor cell biology. *Neuron* **55**, 365–376.

Inoue M., Tokuyama S., Nakayamada H. and Ueda H. (1998a) In vivo signal transduction of tetrodotoxin-sensitive nociceptive responses by substance P given into the planta of the mouse hind limb. *Cell. Mol. Neurobiol.* **18**, 555–561.

Inoue M., Kobayashi M., Kozaki S., Zimmer A. and Ueda H. (1998b) Nociceptin/orphanin FQ-induced nociceptive responses through substance P release from peripheral nerve endings in mice. *Proc. Natl Acad. Sci. USA* **95**, 10949–10953.

Inoue M., Kawashima T., Allen R. G. and Ueda H. (2003a) Nocistatin and prepro-nociceptin/orphanin FQ 160-187 cause nociception through activation of Gi/o in capsaicin-sensitive and of Gs in capsaicin-insensitive nociceptors, respectively. *J. Pharmacol. Exp. Ther.* **306**, 141–146.

Inoue M., Rashid M. H., Kawashima T., Matsumoto M., Maeda T., Kishioka S. and Ueda H. (2003b) The algogenic-induced nociceptive flexion test in mice: studies on sensitivity of the test and stress on animals. *Brain Res. Bull.* **60**, 275–281.

Inoue M., Kawashima T., Takeshima H., Calo G., Inoue A., Nakata Y. and Ueda H. (2003c) In vivo pain-inhibitory role of nociceptin/orphanin FQ in spinal cord. *J. Pharmacol. Exp. Ther.* **305**, 495–501.

Inoue M., Rashid M. H., Fujita R., Contos J. J., Chun J. and Ueda H. (2004) Initiation of neuropathic pain requires lysophosphatidic acid receptor signaling. *Nat. Med.* **10**, 712–718.

Inoue M., Yamaguchi A., Kawakami M., Chun J. and Ueda H. (2006) Loss of spinal substance P pain transmission under the condition of LPA1 receptor-mediated neuropathic pain. *Mol. Pain* **2**, 25.

Ji R. R., Kohno T., Moore K. A. and Woolf C. J. (2003) Central sensitization and LTP: do pain and memory share similar mechanisms? *Trends Neurosci.* **26**, 696–705.

Kim C. H., Oh Y., Chung J. M. and Chung K. (2001) The changes in expression of three subtypes of TTX sensitive sodium channels in sensory neurons after spinal nerve ligation. *Brain Res. Mol. Brain Res.* **95**, 153–161.

Lawson S. N. and Waddell P. J. (1991) Soma neurofilament immunoreactivity is related to cell size and fibre conduction velocity in rat primary sensory neurons. *J. Physiol.* **435**, 41–63.

Lewinter R. D., Skinner K., Julius D. and Basbaum A. I. (2004) Immunoreactive TRPV-2 (VRL-1), a capsaicin receptor homolog, in the spinal cord of the rat. *J. Comp. Neurol.* **470**, 400–408.

Liu W. T., Han Y., Li H. C., Adams B., Zheng J. H., Wu Y. P., Henkemeyer M. and Song X. J. (2009) An in vivo mouse model of long-term potentiation at synapses between primary afferent C-fibers and spinal dorsal horn neurons: essential role of EphB1 receptor. *Mol. Pain* **5**, 29.

Lopshire J. C. and Nicol G. D. (1998) The cAMP transduction cascade mediates the prostaglandin E2 enhancement of the capsaicin-elicited current in rat sensory neurons: whole-cell and single-channel studies. *J. Neurosci.* **18**, 6081–6092.

Matsumoto M., Inoue M., Hald A., Yamaguchi A. and Ueda H. (2006) Characterization of three different sensory fibers by use of neonatal capsaicin treatment, spinal antagonism and a novel electrical stimulation-induced paw flexion test. *Mol. Pain* **2**, 16.

Matsumoto M., Xie W., Inoue M. and Ueda H. (2007) Evidence for the tonic inhibition of spinal pain by nicotinic cholinergic transmission through primary afferents. *Mol. Pain* **3**, 41.

Matsumoto M., Xie W., Ma L. and Ueda H. (2008) Pharmacological switch in Abeta-fiber stimulation-induced spinal transmission in mice with partial sciatic nerve injury. *Mol. Pain* **4**, 25.

Nakagawa H. and Hiura A. (2006) Capsaicin, transient receptor potential (TRP) protein subfamilies and the particular relationship between capsaicin receptors and small primary sensory neurons. *Anat. Sci. Int.* **81**, 135–155.

Rasband M. N., Park E. W., Vanderah T. W., Lai J., Porreca F. and Trimmer J. S. (2001) Distinct potassium channels on pain-sensing neurons. *Proc. Natl Acad. Sci. USA* **98**, 13373–13378.

Rashid M. H., Inoue M., Kondo S., Kawashima T., Bakoshi S. and Ueda H. (2003) Novel expression of vanilloid receptor 1 on capsaicin-insensitive fibers accounts for the analgesic effect of capsaicin cream in neuropathic pain. *J. Pharmacol. Exp. Ther.* **304**, 940–948.

Rashid M. H., Inoue M., Matsumoto M. and Ueda H. (2004) Switching of bradykinin-mediated nociception following partial sciatic nerve injury in mice. *J. Pharmacol. Exp. Ther.* **308**, 1158–1164.

Snider W. D. and McMahon S. B. (1998) Tackling pain at the source: new ideas about nociceptors. *Neuron* **20**, 629–632.

Song X. J., Wang Z. B., Gan Q. and Walters E. T. (2006) cAMP and cGMP contribute to sensory neuron hyperexcitability and hyperalgesia in rats with dorsal root ganglia compression. *J. Neurophysiol.* **95**, 479–492.

Takasu M. A., Dalva M. B., Zigmond R. E. and Greenberg M. E. (2002) Modulation of NMDA receptor-dependent calcium influx and gene expression through EphB receptors. *Science* **295**, 491–495.

Tate S., Benn S., Hick C. *et al.* (1998) Two sodium channels contribute to the TTX-R sodium current in primary sensory neurons. *Nat. Neurosci.* **1**, 653–655.

Ueda H. (1999) In vivo molecular signal transduction of peripheral mechanisms of pain. *Jpn. J. Pharmacol.* **79**, 263–268.

Ueda H. (2006) Molecular mechanisms of neuropathic pain-phenotypic switch and initiation mechanisms. *Pharmacol. Ther.* **109**, 57–77.

Ueda H. (2008) Peripheral mechanisms of neuropathic pain-involvement of lysophosphatidic acid receptor-mediated demyelination. *Mol. Pain* **4**, 11.

Ueda H. and Inoue M. (2000) In vivo signal transduction of nociceptive response by kyotorphin (tyrosine-arginine) through Galpha(i)- and inositol trisphosphate-mediated Ca(2+) influx. *Mol. Pharmacol.* **57**, 108–115.

Urena P., Kong X. F., Abou-Samra A. B., Juppner H., Kronenberg H. M., Potts J. T. Jr and Segre G. V. (1993) Parathyroid hormone (PTH)/PTH-related peptide receptor messenger ribonucleic acids are widely distributed in rat tissues. *Endocrinology* **133**, 617–623.

Usdin T. B., Gruber C. and Bonner T. I. (1995) Identification and functional expression of a receptor selectively recognizing parathyroid hormone, the PTH2 receptor. *J. Biol. Chem.* **270**, 15455–15458.

Usdin T. B., Hoare S. R., Wang T., Mezey E. and Kowalak J. A. (1999a) TIP39: a new neuropeptide and PTH2-receptor agonist from hypothalamus. *Nat. Neurosci.* **2**, 941–943.

Usdin T. B., Hilton J., Vertesi T., Harta G., Segre G. and Mezey E. (1999b) Distribution of the parathyroid hormone 2 receptor in rat: immunolocalization reveals expression by several endocrine cells. *Endocrinology* **140**, 3363–3371.

Usdin T. B., Dobolyi A., Ueda H. and Palkovits M. (2003) Emerging functions for tuberoinfundibular peptide of 39 residues. *Trends Endocrinol. Metab.* **14**, 14–19.

Wang T., Palkovits M., Rusnak M., Mezey E. and Usdin T. B. (2000) Distribution of parathyroid hormone-2 receptor-like immunoreactivity and messenger RNA in the rat nervous system. *Neuroscience* **100**, 629–649.

0022-3565/10/3332-540–546$20.00
THE JOURNAL OF PHARMACOLOGY AND EXPERIMENTAL THERAPEUTICS
Copyright © 2010 by The American Society for Pharmacology and Experimental Therapeutics
JPET 333:540–546, 2010

Vol. 333, No. 2
164830/3576474
Printed in U.S.A.

Evidence for De Novo Synthesis of Lysophosphatidic Acid in the Spinal Cord through Phospholipase A_2 and Autotaxin in Nerve Injury-Induced Neuropathic Pain

Lin Ma, Hitoshi Uchida, Jun Nagai, Makoto Inoue, Junken Aoki, and Hiroshi Ueda

Division of Molecular Pharmacology and Neuroscience, Nagasaki University Graduate School of Biomedical Sciences, Nagasaki, Japan (L.M., H.Uc., J.N., M.I., H.Ue.); and Laboratory of Molecular and Cellular Biochemistry, Graduate School of Pharmaceutical Sciences, Tohoku University, Sendai, Japan (J.A.)

Received December 14, 2009; accepted January 29, 2010

ABSTRACT

We previously reported that lysophosphatidic acid (LPA) initiates nerve injury-induced neuropathic pain and its underlying mechanisms. In addition, we recently demonstrated that intrathecal injection of LPA induces de novo LPA production through the action of autotaxin (ATX), which converts lysophosphatidylcholine to LPA. Here, we examined nerve injury-induced de novo LPA production by using a highly sensitive biological titration assay with B103 cells expressing LPA_1 receptors. Nerve injury caused high levels of LPA production in the ipsilateral sides of the spinal dorsal horn and dorsal roots, but not in the dorsal root ganglion, spinal nerve, or sciatic nerve. Nerve injury-induced LPA production reached its maximum at 3 h after injury, followed by a rapid decline by 6 h. The LPA production was significantly attenuated in ATX heterozygous mutant mice, whereas the concentration and activity of ATX in cerebrospinal fluid were not affected by nerve injury. On the other hand, the activities of cytosolic phospholipase A_2 ($cPLA_2$) and calcium-independent phospholipase A_2 ($iPLA_2$) were enhanced, with peaks at 1 h after injury. Both de novo LPA production and neuropathic pain-like behaviors were substantially abolished by intrathecal injection of arachidonyl trifluoromethyl ketone, a mixed inhibitor of $cPLA_2$ and $iPLA_2$, or bromoenol lactone, an $iPLA_2$ inhibitor, at 1 h after injury. However, administration of these inhibitors at 6 h after injury had no significant effect on neuropathic pain. These findings provide evidence that PLA_2- and ATX-mediated de novo LPA production in the early phase is involved in nerve injury-induced neuropathic pain.

Lysophosphatidic acid (LPA) is a bioactive lipid mediator that exerts a variety of biological activities, including promotion of cell proliferation, prevention of apoptosis, and modulation of cell shape and cell migration (Aoki, 2004; Aoki et al., 2008). Consequently, LPA has been demonstrated to play important roles in numerous pathological and physiological situations, such as wound healing, lung fibrosis, cancer, reproduction, and hair growth (Balazs et al., 2001; Mills and Moolenaar, 2003; Ye et al., 2005; Pasternack et al., 2008; Tager et al., 2008). Moreover, LPA has been detected in several biological fluids, including serum, saliva, seminal fluid, follicular fluid, and even ascites from ovarian cancer patients (Xu et al., 1995; Tokumura et al., 1999; Aoki et al., 2002; Hama et al., 2002; Sugiura et al., 2002). Furthermore, LPA is a lipid metabolite that is produced after tissue injury (Eichholtz et al., 1993; Tigyi et al., 1995).

Previously, we reported that LPA_1 receptor signaling initiated nerve injury-induced neuropathic pain and its underlying machineries, including demyelination and altered expressions of pain-related molecules (Inoue et al., 2004; Ueda, 2006, 2008). In addition, nerve injury-induced neuropathic pain could be caused by a single intrathecal injection of LPA and blocked by LPA_1 receptor knockdown at the early, but not late, stage (Inoue et al., 2004). Moreover, deletion of the

This work was supported by Special Coordination Funds from the Science and Technology Agency of the Japanese Government, Grants-in-Aid from the Ministry of Education, Science, Culture, and Sports of Japan and the Human Frontier Science Program, and Health Labor Sciences Research Grants from the Ministry of Health, Labor, and Welfare of Japan (to H.Ue.) for Research on Allergic Disease and Immunology and Third-Term Comprehensive Control Research for Cancer (398-49).

Article, publication date, and citation information can be found at http://jpet.aspetjournals.org.

doi:10.1124/jpet.109.164830.

ABBREVIATIONS: LPA, lysophosphatidic acid; ATX, autotaxin; LPC, lysophosphatidylcholine; $atx^{+/-}$, ATX gene heterozygous mutant mice; WT, wild type; AACOCF3, arachidonyl trifluoromethyl ketone; BEL, bromoenol lactone; DMEM, Dulbecco's modified Eagle's medium; SC, dorsal horn of the lumbar spinal cord; DR, dorsal root; DRG, dorsal root ganglion; SPN, spinal nerve; SCN, sciatic nerve; B103(+), LPA_1 receptor-expressing B103 cells; CSF, cerebrospinal fluid; PLA, phospholipase A; $cPLA_2$, cytosolic phospholipase A_2; $iPLA_2$, calcium-independent phospholipase A_2; PC, phosphatidylcholine; B103(−), LPA_1 receptor-lacking B103 cells; IC_{50}, half-maximal inhibitory concentration; NK1, neurokinin 1; NMDA, *N*-methyl-D-aspartate; SP, substance P.

LPA_1 receptor gene did not change the basal nociceptive threshold (Inoue et al., 2004), thus providing evidence that nerve injury-induced neuropathic pain is initiated by de novo LPA synthesis via defined biosynthetic pathways (Aoki, 2004; Aoki et al., 2008). Very recently, we found that intrathecal administration of LPA caused feed-forward LPA production at the early phase (Ma et al., 2009b). Based on these findings, we speculate that nerve injury may induce the production of LPA at the early phase and subsequently cause LPA_1 receptor activation to induce neuropathic pain. Moreover, we previously demonstrated that autotaxin (ATX), which converts lysophosphatidylcholine (LPC) to LPA (Aoki, 2004; Aoki et al., 2008), is involved in nerve injury-induced neuropathic pain, because neuropathic pain was significantly attenuated in ATX gene heterozygous mutant ($atx^{+/-}$) mice (Inoue et al., 2008a). In addition, LPC conversion to LPA mediated by ATX has been implicated in LPA-induced LPA production (Ma et al., 2009b). We also found that intense stimulation of spinal cord slices with combined pain transmitters or capsaicin, which is thought to induce the release of pain transmitters, caused biosynthesis of LPC, which was subsequently converted to LPA by ATX (Inoue et al., 2008b). Taken together, these findings suggest that nerve injury-induced neuropathic pain occurs after LPC production, with subsequent LPA production via LPC conversion by ATX and activation of LPA_1 receptor signaling. The present study represents an initial neurochemical examination of the processes underlying nerve injury-induced de novo LPA production and provides evidence of PLA_2- and ATX-mediated early biosynthesis of LPA after nerve injury.

Materials and Methods

Animals. Male C57BL/6J mice (Tagawa Experimental Animal Laboratory, Nagasaki, Japan), $atx^{+/-}$ mice (Tanaka et al., 2006), and their sibling wild-type (WT) mice from the same genetic background were used in this study. The mice weighed 20 to 24 g. They were kept in a room maintained at 21 ± 2°C and 55 ± 5% relative humidity with a 12-h/12-h light/dark cycle and had free access to a standard laboratory diet and tap water. The procedures were approved by the Nagasaki University Animal Care Committee and complied with the fundamental guidelines for the proper conduct of animal experiments and related activities in academic research institutions under the jurisdiction of the Ministry of Education, Culture, Sports, Science, and Technology of Japan.

Drugs. LPC was purchased from Sigma-Aldrich (St. Louis, MO). Arachidonyl trifluoromethyl ketone (AACOCF3) and bromoenol lactone (BEL) were purchased from Cayman Chemical (Ann Arbor, MI). For in vitro experiments, LPC was dissolved in Dulbecco's modified Eagle's medium (DMEM) containing 0.1% fatty acid-free bovine serum albumin (Sigma-Aldrich). For in vivo experiments, AACOCF3 and BEL were dissolved in artificial cerebrospinal fluid (125 mM NaCl, 3.8 mM KCl, 1.2 mM KH_2PO_4, 26 mM $NaHCO_3$, 10 mM glucose).

Partial Sciatic Nerve Ligation. Partial ligation of the sciatic nerves was performed under anesthesia with pentobarbital (50 mg/kg, i.p.), according to modified methods (Rashid et al., 2003). The common sciatic nerve of the right hind limb was exposed at the high thigh level through a small incision, and the dorsal half of the nerve thickness was tightly ligated with a silk suture. A sham operation was performed similarly except without touching the sciatic nerve.

Sample Preparation from Tissues. At different time points after sciatic nerve injury, mice were anesthetized with pentobarbital (50 mg/kg, i.p.) as reported previously (Ma et al., 2009b). The unilateral dorsal horn (laminae I-V) of the lumbar (L4–L6) spinal cord (SC), L4–L6 dorsal roots (DRs), L4–L6 dorsal root ganglions (DRGs), L4–L6 spinal nerves (SPNs), and L4–L6 sciatic nerves (SCNs) on the ipsilateral or contralateral side were then removed to enable the extraction of LPA, as shown in Fig. 1A. The average wet weights of the isolated unilateral SCs, DRs, DRGs, SPNs, and SCN in each mouse were 4, 2, 2, 2, and 2.5 mg, respectively. After their isolation, the tissue samples were placed in 1.5-ml polypropylene tubes and homogenized by sonication in 300 μl of serum-free DMEM for approximately 30 s. To extract LPA from the homogenates using a solid-phase lipid extraction method, the samples were slowly loaded onto Oasis HLB cartridges (Millipore Corporation, Tokyo, Japan), which had been preconditioned with 3 ml of methanol followed by 3 ml of distilled water. The columns were then washed with 3 ml of distilled water and 1 ml of chloroform. Subsequently, LPA was eluted with 600 μl of methanol and dried with N_2 gas. The final samples were dissolved in 100 μl of DMEM and stored at −80°C until analysis.

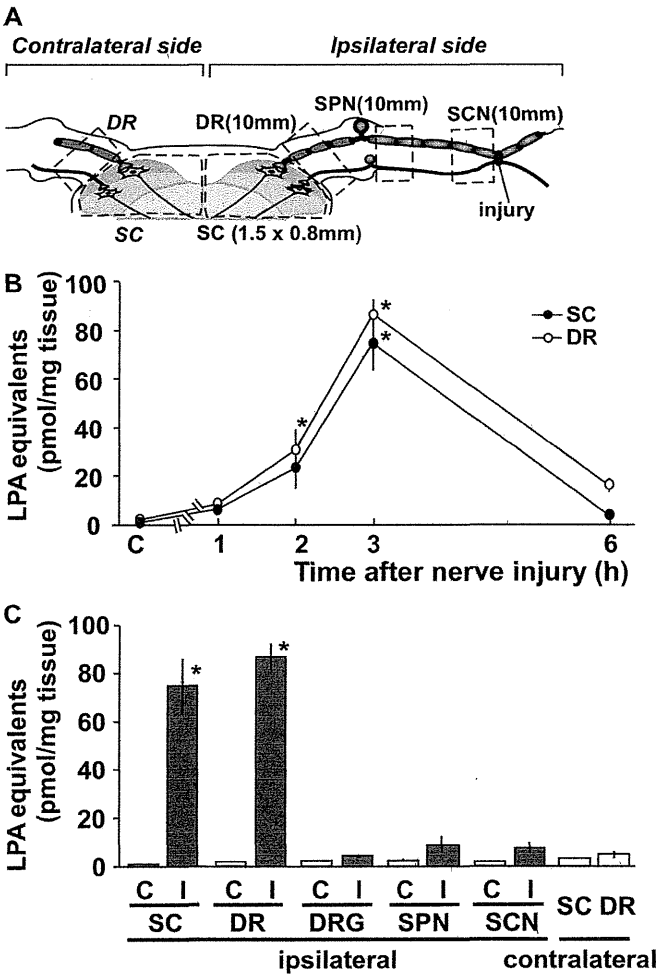

Fig. 1. Nerve injury-induced de novo LPA production in the ipsilateral sides of the spinal dorsal horn and dorsal roots. (A) Exact locations of the removed samples, including the dorsal horn of the lumbar spinal cord (SC), dorsal roots (DR), dorsal root ganglions (DRG), spinal nerves (SPN), and sciatic nerves (SCN). (B) Quantification of LPA production in the ipsilateral sides of the SC and DR at different time points after sciatic nerve injury. C represents the control group (naive mice). (C) Evaluation of LPA production after nerve injury in different preparations from the ipsilateral sides of the SC, DR, DRG, SPN, and SCN and the contralateral sides of the SC and DR at 3 h postinjury. I represents the injured group. The LPA measurements were carried out in triplicate for each sample. All data represent means ± S.E.M. from three separate experiments. Cell-rounding morphology was evaluated in at least 500 enhanced green fluorescent protein-positive cells. *, $p < 0.05$, versus the control group.

Biological Titration Method. B103 cells expressing LPA_1 receptors and enhanced green fluorescent protein [B103(+) cells] were used for quantitative measurement of LPA, according to a modified method (Inoue et al., 2008b; Ma et al., 2009b) based on an earlier report (Ishii et al., 2000). The cells were maintained as monolayer cultures on tissue culture dishes in DMEM supplemented with 10% heat-inactivated fetal bovine serum (Invitrogen, Carlsbad, CA), penicillin, and streptomycin (final concentrations: 100 U/ml and 100 μg/ml, respectively). Cells were seeded at 2.5×10^4 cells/cm^2 onto eight-well glass slides coated with poly-L-lysine (Sigma-Aldrich; final concentration, 100 mg/l) and collagen (BD Bioscience, San Jose, CA; final concentration, 5 μg/cm^2). The cells were then cultured in DMEM containing 10% heat-inactivated fetal bovine serum at 37°C in a 5% CO_2 atmosphere for 10 h. Subsequently, the cells were cultured in serum-starved DMEM for 15 h.

In the biological assay, a standard LPA solution or a diluted tissue sample was applied to B103(+) cells. After incubation at 37°C for 20 min, the medium was replaced with 4% paraformaldehyde followed by incubation at 25°C for 60 min. The glass slide was then coverslipped with Fluoromount (DBS, Pleasanton, CA) and examined under a fluorescence microscope (Keyence, Osaka, Japan). The percentage of cells exhibiting a rounded morphology among at least 500 cells in each well was determined.

Collection of Cerebrospinal Fluid. Cerebrospinal fluid (CSF) was collected according to a previously described method (Inoue et al., 2008b). In this method, mice were anesthetized with pentobarbital (50 mg/kg, i.p.), and the L4–L5 vertebral column was carefully exposed. Next, SP8 polyethylene tubing (i.d.: 0.20 mm; o.d.: 0.50 mm; Natsume, Tokyo, Japan) connected to a syringe was inserted into the subarachnoid space of the exposed L4–L5 vertebral column, and the CSF was suctioned by using the syringe.

Western Blotting. Western blotting analysis for ATX was performed as reported previously (Inoue et al., 2008b). In brief, CSF was collected at 2 h after nerve injury or sham operation. The collected CSF (0.5 μl) was applied to an SDS-polyacrylamide gel (8%). An anti-ATX antibody described in a previous report (Tanaka et al., 2006) was used at a dilution of 1:100. A horseradish peroxidase-conjugated anti-rat antibody (Zymed Laboratories, South San Francisco, CA) was used as the secondary antibody at a dilution of 1:1000. Immunoreactive bands were detected by using an enhanced chemiluminescent substrate (SuperSignal West Pico Chemiluminescent Substrate; Pierce Chemical, Rockford, IL) for horseradish peroxidase. The intensities of the immunoreactive bands were analyzed by NIH Imaging for Macintosh.

Phospholipase A_2 Activity Assays. The activities of cytosolic phospholipase A_2 ($cPLA_2$) and calcium-independent phospholipase A_2 ($iPLA_2$) were detected by using the following assays as described previously (Smani et al., 2003). In brief, at different time points after sciatic nerve injury, mice were anesthetized with pentobarbital (50 mg/kg i.p.), and the ipsilateral side of the spinal dorsal horn was removed. After sonication and centrifugation at 20,000*g* for 20 min at 4°C, the supernatant was collected and kept on ice. The protein concentration of the supernatant was determined by the Lowry method, and the assays were performed on the same day by using a $cPLA_2$ assay kit (Cayman Chemical) to evaluate the $cPLA_2$ activity or a modified $cPLA_2$ assay kit (Cayman Chemical) to evaluate the $iPLA_2$ activity, as described previously (Smani et al., 2003). In the $cPLA_2$ assay, the tissue samples were incubated with both BEL, an $iPLA_2$ inhibitor (Ackermann et al., 1995), and a substrate, arachidonoyl thio-PC, at 20°C for 1 h in a assay buffer. The reactions were stopped by 5,5′-dithiobis-(2-nitrobenzoic acid)/EGTA for 5 min, and the absorbances were determined at 405 nm by using a standard plate reader. To detect the activity of $iPLA_2$, but not $cPLA_2$, the samples were incubated with the substrate arachidonoyl thio-PC at 20°C for 1 h in a modified Ca^{2+}-free buffer [4 mM EGTA, 160 mM HEPES (pH 7.4), 300 mM NaCl, 8 mM Triton X-100, 60% glycerol, 2 mg/ml bovine serum albumin]. The reactions were stopped by the addition of 5,5′-dithiobis(nitrobenzoic acid) for 5 min. The activity of PLA_2 was defined as the percentage of the control activity as follows: injured tissues (absorbance/mg of protein)/normal tissues (absorbance/mg of protein) × 100.

Intrathecal Injection. The intrathecal injection was carried out as reported previously (Ma et al., 2009a) according to the modified method (Hylden and Wilcox, 1980). In this method, an unanesthetized mouse was held by the pelvic girdle in one hand, and the syringe was held in another hand. The needle was inserted into the tissue between the dorsal aspects of lumbar regions five and six, at an angle of approximately 20° above the vertebral column, then it slipped into the groove between the spinous and transverse processes. Changing the angle of the syringe to 10°, the needle was carefully moved forward to the intervertebral space, and 5 μl of drug solution was injected. The whole operation was performed within 1 min. After injection, no specific behavior or sign of distress was observed in the injected mouse.

Nociceptive Tests. In thermal paw withdrawal tests, nociception was measured as the latency to paw withdrawal evoked by exposure to a thermal stimulus (Hargreaves et al., 1988; Rashid et al., 2003; Ma et al., 2009a). Unanesthetized animals were placed in Plexiglas cages on top of a glass sheet and allowed an adaptation period of 1 h. A thermal stimulator (IITC Inc., Woodland Hills, CA) was positioned under the glass sheet, and the focus of the projection bulb was aimed precisely at the middle of the plantar surface of the animal. A mirror attached to the stimulator permitted visualization of the plantar surface. A cutoff time of 20 s was set to prevent tissue damage.

The paw pressure test was performed as described previously (Rashid et al., 2003; Ma et al., 2009a). Mice were placed in a Plexiglas chamber on a 6 × 6-mm wire mesh grid floor and allowed to acclimatize for 1 h. A mechanical stimulus was then delivered to the middle of the plantar surface of the right hind paw by using a Transducer Indicator (model 1601; IITC Inc.). The pressure required to induce a flexor response was defined as the pain threshold. All behavioral experiments were performed under double-blinded conditions.

Statistical Analysis. Statistical analyses were carried out with Student's *t* test and Tukey's multiple comparison post hoc analysis after one-way analysis of variance. The criterion of significance was set at $p < 0.05$. All results are expressed as means ± S.E.M.

Results

Nerve Injury-Induced de Novo LPA Production in the Ipsilateral Sides of the Spinal Dorsal Horn and Dorsal Roots. To quantify LPA production after sciatic nerve injury, we developed a biological titration method using LPA_1 receptor-expressing B103 cells [B103(+) cells], based on previously described methods (Ishii et al., 2000; Inoue et al., 2008b; Ma et al., 2009b). Using our method, we evaluated the percentages of cells showing a rounded morphology induced by the addition of LPA and examined at least 500 cells in each well. The measurements were specific for LPA, because high levels of both LPC and S1P were reported to have no effect on these cells (Inoue et al., 2008b; Ma et al., 2009b). In addition, our most recent study demonstrated that LPA did not induce any morphological rounding of B103 cells lacking LPA_1 receptor expression [B103(−) cells], even if LPA was present at a high concentration (Ma et al., 2009b). In the present study using B103(+) cells, the calibration curve for the LPA-induced cell-rounding activity was linear as the LPA concentration increased from 0.15 to 5 pmol, after subtracting the basal cell-rounding activity. Experiments were carried out in 100-μl wells. The equation was defined as $y = 5.454x + 5.66$ ($R^2 = 0.991$; x: $\log_{10}$[LPA (pmol)]; y: percentage of rounded cells). In subsequent exper-

iments, LPA equivalents for the tissue extracts of the different regions were estimated by using this equation based on the linear LPA concentration-dependent responses, as mentioned in our recent report (Ma et al., 2009b).

As shown in Fig. 1B, the basal level of LPA equivalents in the SCs of control mice was 0.79 pmol/mg tissue. However, the LPA levels increased in a time-dependent manner in the ipsilateral side of the SC after sciatic nerve injury. The maximal production (74.8 pmol/mg tissue) was obtained at 3 h after nerve injury and substantially disappeared by 6 h. Increases in the nerve injury-induced LPA level were also observed in the ipsilateral side of the DR with a similar time course (Fig. 1B). In contrast, no significant increases in the LPA level were observed in the ipsilateral side of the DRG, SPN, or SCN at 3 h after injury (Fig. 1C). In addition, no LPA increases were observed in the contralateral side of the SC or DR at 3 h after nerve injury (Fig. 1C), suggesting that the newly produced LPA is unlikely to diffuse throughout the CSF.

ATX Involvement in Nerve Injury-Induced LPA Production. The LPA levels in $atx^{+/-}$ mice at 3 h after nerve injury were evaluated. The LPA levels were significantly attenuated in the ipsilateral sides of the SC and DR in $atx^{+/-}$ mice compared with WT mice (Fig. 2).

Lack of Nerve Injury-Induced Changes in the Concentration and Activity of ATX in CSF. To examine whether the concentration or enzyme activity of ATX in CSF was affected by nerve injury, we collected CSF from mice at 2 h after nerve injury or sham operation. In a Western blot analysis for ATX, there were no differences in the ATX amounts in CSF (0.5 μl) between the presence and absence of nerve injury (Fig. 3A). In addition, when the CSF (0.5 μl) was incubated with LPC (10 pmol) for 30 min, there were no significant changes in the LPA equivalents between these preparations in the biological titration assay (Fig. 3B). These findings suggest that the concentration and enzyme activity of ATX are not affected by nerve injury.

Nerve Injury-Induced Activation of Spinal $cPLA_2$ and $iPLA_2$ at the Early Stage. We attempted to evaluate the signal transduction pathway leading to LPA production. Because the enzymes $cPLA_2$ and $iPLA_2$, which are expressed in the spinal cord (Karin Killermann et al., 2005), catalyze phosphatidylcholine (PC) conversion to LPC (Aoki, 2004; Aoki et al., 2008; Inoue et al., 2008b), the ipsilateral side of the SC in injured or control mice was collected and analyzed

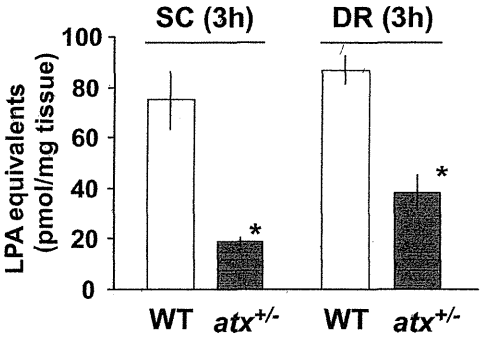

Fig. 2. ATX involvement in nerve injury-induced LPA production. Quantification of LPA production in the SC and DR of injured WT mice and $atx^{+/-}$ mice at 3 h postinjury. The LPA measurements were carried out in triplicate for each sample. All data represent means ± S.E.M. from three separate experiments. *, $p < 0.05$, versus the WT group.

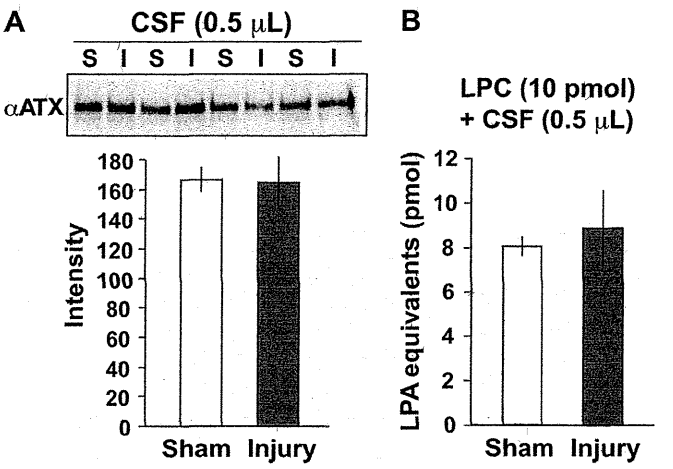

Fig. 3. Lack of nerve injury-induced changes in the concentration and activity of ATX in CSF. CSF was collected at 2 h after nerve injury or sham operation, and the concentration and enzyme activity of ATX in CSF (0.5 μl) was analyzed by Western blotting (A) and a biological titration method (B). All data represent means ± S.E.M.

by $cPLA_2$ and $iPLA_2$ activity assays. As shown in Fig. 4A, the $cPLA_2$ activity was significantly increased at 1 h after nerve injury compared with the control group, and the increase was followed by remarkable declines at 3 and 6 h after injury. A significant increase in the $iPLA_2$ activity was also observed at 1 h after injury, but only slight decreases were observed at 3 and 6 h after injury (Fig. 4B).

Nerve Injury-Induced LPA Production Through PLA_2. To assess the roles of $cPLA_2$ and $iPLA_2$ in the nerve injury-induced LPA production, AACOCF3, a mixed inhibitor of $cPLA_2$ and $iPLA_2$ (Street et al., 1993; Ackermann et al., 1995), or BEL, an $iPLA_2$ inhibitor (Ackermann et al., 1995), was administered (10 nmol i.t.) at 1 h after injury. At 3 h after injury, the ipsilateral sides of the SC and DR were removed to measure the LPA levels. The nerve injury-induced LPA productions in the SC and DR were significantly blocked by postinjury treatment with AACOCF3 (Fig. 5A). Similar results were found in the BEL treatment group (Fig. 5B).

Blockade of Neuropathic Pain by Early Treatment with PLA_2 Inhibitors. To assess the pharmacological effects of AACOCF3 or BEL in behavioral tests, different doses of AACOCF3 or BEL were administered at 1 h after nerve injury, and nociceptive tests were performed on 3, 5, and 7 days after injury. Sciatic nerve injury caused robust mechan-

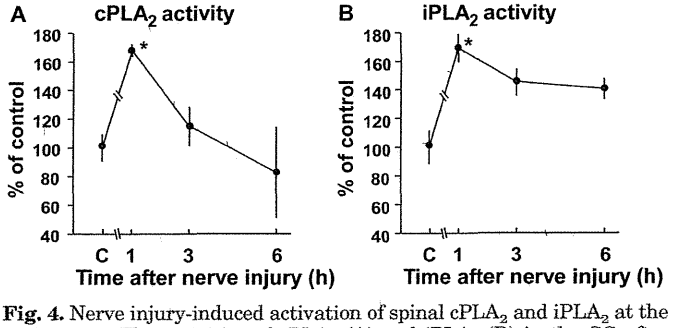

Fig. 4. Nerve injury-induced activation of spinal $cPLA_2$ and $iPLA_2$ at the early stage. The activities of $cPLA_2$ (A) and $iPLA_2$ (B) in the SC after nerve injury were determined by $cPLA_2$ and $iPLA_2$ activity assays. C represents the control group (naive mice). All data represent means ± S.E.M. from three to five separate experiments. *, $p < 0.05$ versus the control group.

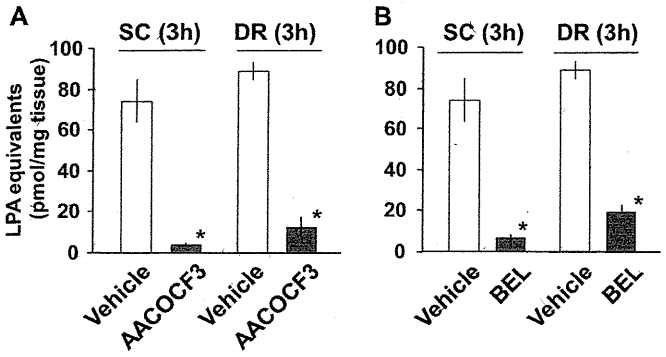

Fig. 5. Nerve injury-induced LPA production through PLA_2. AACOCF3 (A) or BEL (B) was administered (10 nmol i.t.) at 1 h postinjury, and the ipsilateral sides of the SC and DR were removed at 3 h postinjury to evaluate the LPA levels. The LPA measurements were carried out in triplicate for each sample. All data represent means ± S.E.M. from three separate experiments. *, $p < 0.05$, versus the vehicle group.

ical allodynia at 3 days after nerve injury in the ipsilateral side, and the allodynia was blocked by intrathecal injection of AACOCF3 or BEL at 1 h after injury in a dose-dependent manner, whereas no effects on the nociceptive thresholds of the contralateral side were observed (Fig. 6, A and B). Because the maximal effect of AACOCF3 or BEL was observed at 10 nmol, we adopted this dose in subsequent experiments. However, no abnormal behaviors were observed after AACOCF3 or BEL treatment at 10 or 30 nmol. As shown in Fig. 6, C and D, sciatic nerve injury-induced thermal hyperalgesia and mechanical allodynia lasted for at least 7 days in the ipsilateral side, and these neuropathic pain behaviors were significantly attenuated by postinjury treatment with AACOCF3 or BEL at 10 nmol, whereas no differences were observed in the contralateral side.

To evaluate the critical time period for the antagonistic effects of AACOCF3 and BEL, they were each administered (10 nmol i.t.) at 6 h postinjury. In accordance with the above time course, nociceptive tests were performed on 3, 5, and 7 days after injury. However, neither of the inhibitors had any effects on nerve injury-induced thermal and mechanical neuropathic pain (Fig. 7).

Discussion

In the present study, we have demonstrated for the first time that sciatic nerve injury causes de novo synthesis of LPA in vivo by the action of endogenous ATX, using a previously described method (Inoue et al., 2008b; Ma et al., 2009b). This method, in which LPA_1 receptor-mediated cell-rounding activity was measured as a quantitative evaluation of the LPA levels in processed extracts from tissue samples, has been confirmed to be a highly sensitive and specific assay for the evaluation of low levels of LPA in extracts (Inoue et al., 2008b; Ma et al., 2009b), because LPA concentration was detectable from 0.15 pmol (equivalent: 1.5 nM) in this assay, showing the higher sensitivity compared with the enzymatic cycling method, another widely used method for LPA determination that is only suitable for concentrations over 100 nM LPA (Kishimoto et al., 2003). It should be noted that the LPA levels in the SCs and DRs of control mice were negligible (0.79 and 1.81 pmol/mg tissue, respectively). When the sciatic nerve was injured, the LPA levels were elevated by 95- and 48-fold (74.8 and 86.9 pmol/mg tissue, respectively) in these regions at 3 h on the ipsilateral

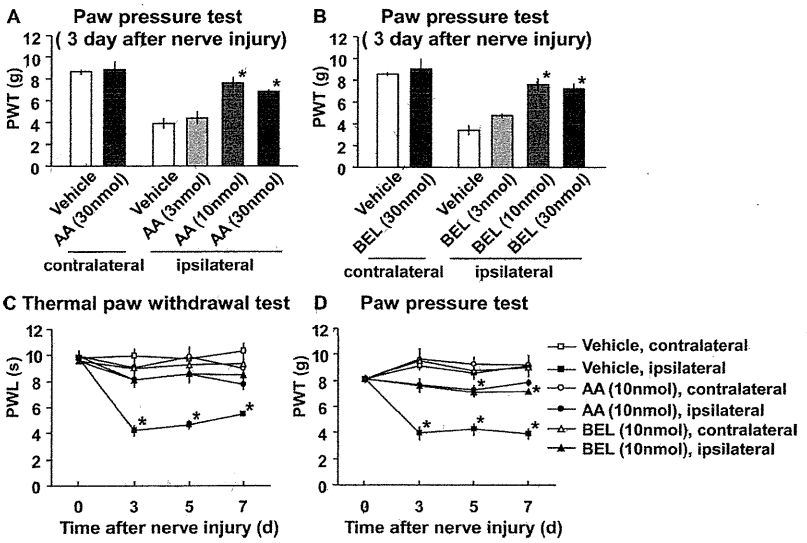

Fig. 6. Blockade of neuropathic pain by early treatment with PLA_2 inhibitors. A and B, difference doses of AACOCF3 (A) or BEL (B) were administered intrathecally at 1 h postinjury, and the paw pressure test was performed at 3 days postinjury. C and D, AACOCF3 or BEL was administered (10 nmol i.t.) at 1 h postinjury. Thermal paw withdrawal tests (C) and paw pressure tests (D) were performed at days 3, 5, and 7 after injury. The results represent the thresholds of the latency (in s) or pressure (in g) to thermal or mechanical stimulation, respectively. PWL, paw withdrawal latency; PWT, paw withdrawal threshold. All data represent means ± S.E.M. from three or four mice. *, $p < 0.05$, versus the vehicle group or contralateral side.

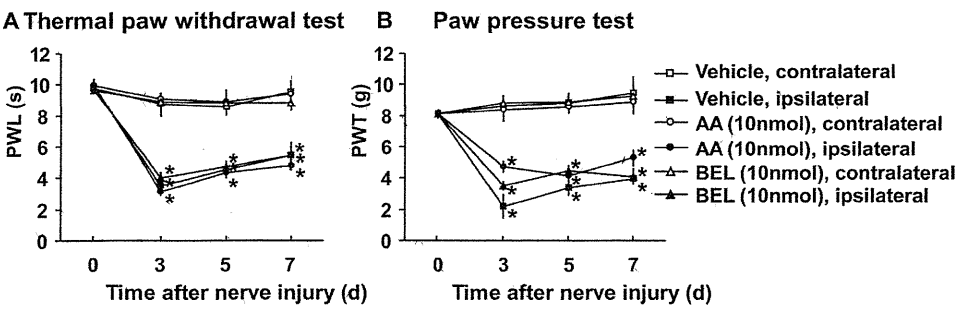

Fig. 7. Delayed treatment with PLA_2 inhibitors has no effect on neuropathic pain. AACOCF3 or BEL was administered (10 nmol i.t.) at 6 h postinjury. Thermal paw withdrawal tests (A) and paw pressure tests (B) were performed at days 3, 5, and 7 after injury. All data represent means ± S.E.M. from three or four mice. *, $p < 0.05$ versus the contralateral side.

side, whereas there was no significant elevation on the contralateral side. This injury-induced production of LPA is consistent with the previous finding that LPA was generated after hemorrhagic brain injury (Tigyi et al., 1995). However, there were no increases in the LPA levels in the ipsilateral DRG, SPN, or SCN, suggesting that LPA production occurs in the spinal cord and migrates to the vicinity of the dorsal root along the nerve fiber (Fig. 8).

Sciatic nerve injury caused time-dependent increases in the LPA levels in the SC and DR that lasted until 3 h postinjury. These elevations may be attributed to the sum of the original de novo LPA production plus the produced LPA-induced feed-forward LPA production (Fig. 8), because we recently reported that a low level of LPA induced feed-forward LPA synthesis through ATX and LPA_3 receptor in both in vivo and in vitro experiments (Ma et al., 2009b). Furthermore, the increased LPA levels were followed by significant decreases at 6 h after injury. These decreases may be caused by end-product inhibition of ATX, because ATX activity is inhibited by high levels of LPA (van Meeteren et al., 2005).

Two major pathways of LPA production have been proposed, namely intracellular LPA generation from phosphatidic acid by phospholipase A_1 or PLA_2 and extracellular generation from LPC by ATX (Aoki, 2004; Aoki et al., 2008). However, based on the observations that both stimulation-induced LPA synthesis and LPA-induced LPA production absolutely required the presence of ATX in in vitro studies using spinal cord slices (Inoue et al., 2008b; Ma et al., 2009b), the latter pathway seems to be more important for the de novo synthesis of LPA in the spinal cord after nerve injury. Indeed, a significant level of ATX is present in CSF (Sato et al., 2005; Inoue et al., 2008b). In the present study, $atx^{+/-}$ mice exhibited significant attenuation of nerve injury-induced LPA production at 3 h after injury, and this finding is consistent with our previous observation that there was a partial, but significant, attenuation of nerve injury-induced neuropathic pain in $atx^{+/-}$ mice (Inoue et al., 2008a). Therefore, it is evident that nerve injury-induced de novo LPA production largely depends on the action of ATX in CSF in vivo. On the other hand, in the present study, we found that the concentration and activity of ATX in CSF were not changed by nerve injury, indicating that LPC biosynthesis is the rate-limiting process for de novo biosynthesis of LPA after nerve injury. Taken together, these findings suggest that the rapid production of LPA after injury can be attributed to the more rapid LPC production and subsequent ATX-mediated conversion of LPC to LPA. Experiments using an ATX inhibitor may support this hypothesis. However, because the commercially available ATX inhibitor shows some affinity for the LPA_3 receptor, which is involved in LPA-induced LPA production (Ma et al., 2009b), we should wait for a specific ATX inhibitor to be available.

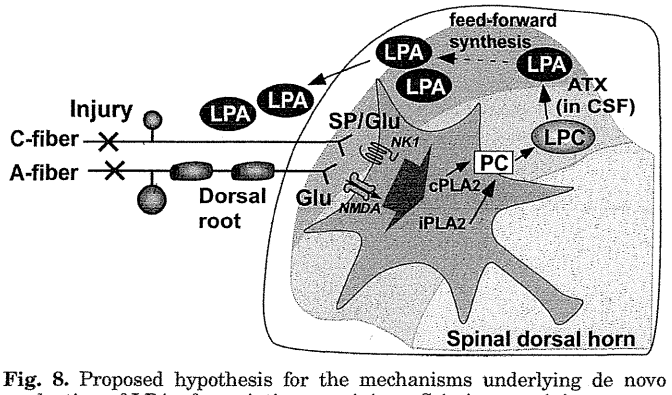

Fig. 8. Proposed hypothesis for the mechanisms underlying de novo production of LPA after sciatic nerve injury. Sciatic nerve injury causes intense activation of NK1 and NMDA receptors by substance P (SP) and glutamate (Glu), respectively, leading to subsequent activation of both $cPLA_2$ and $iPLA_2$, which catalyze a conversion of PC to LPC. ATX then converts LPC to LPA, which further induces an LPA production in the ATX and LPA_3 receptor-mediated feed-forward system. The produced LPA in the spinal cord migrates to the vicinity of the dorsal root along the nerve fiber.

In the present study, we attempted to clarify the signal transduction after nerve injury that leads to the de novo biosynthesis of LPC and LPA. Because the enzymes $cPLA_2$ and $iPLA_2$, which are expressed in the spinal cord (Karin Killermann et al., 2005), catalyze PC conversion to LPC (Aoki, 2004; Aoki et al., 2008; Inoue et al., 2008b), we propose that both $cPLA_2$ and $iPLA_2$ are involved in the nerve injury-induced production of LPC and LPA. In fact, we found that the activities of both $cPLA_2$ and $iPLA_2$ were remarkably increased at 1 h postinjury, which is consistent with a previous report that PLA_2 activity was rapidly and significantly elevated after spinal cord injury (Nai-Kui et al., 2006). There is a contradictory report that the activities of both $cPLA_2$ and $iPLA_2$ were not altered by carrageenan-induced inflammatory pain (Karin Killermann et al., 2005). Although the detailed mechanisms underlying this difference remain unclear, it may be attributable to the differences between neuropathic pain and inflammatory pain.

It should be noted that the $cPLA_2$ activation was transient, whereas the $iPLA_2$ activation was sustained for more than 6 h. Considering that the injury-induced LPA production observed in the present study and the LPA_1 receptor signaling-mediated initiation of neuropathic pain in a previous study (Ma et al., 2009a) were terminated within 6 h, $cPLA_2$ seems more likely to be related to the de novo LPA production. Indeed, AACOCF3, a mixed inhibitor of $cPLA_2$ [half-maximal inhibitory concentration (IC_{50}): 2–8 μM] and $iPLA_2$ (IC_{50}: 15 μM) (Street et al., 1993; Ackermann et al., 1995), substantially abolished the nerve injury-induced LPA production and neuropathic pain. However, BEL, a more potent and selective $iPLA_2$ inhibitor (IC_{50}: 60 nM) (Ackermann et al., 1995), also substantially abolished the injury-induced LPA production and neuropathic pain. Therefore, both $iPLA_2$ and $cPLA_2$ are considered to play roles in nerve injury-induced LPA production and neuropathic pain (Fig. 8). The difference between the short-term LPA production within 6 h and the sustained $iPLA_2$ activation for more than 6 h may be explained by end-product inhibition of ATX by LPA (van Meeteren et al., 2005). The roles of $cPLA_2$ and $iPLA_2$ proposed in the present study are also consistent with our recent finding that the activation of both $cPLA_2$ and $iPLA_2$ as the final step caused de novo biosynthesis of LPC from PC after intense stimulation of the primary afferent or simultaneous activation of neurokinin 1 (NK1) and *N*-methyl-D-aspartate (NMDA) receptors by substance P (SP) and glutamate (Glu), respectively (Inoue et al., 2008b) (Fig. 8). Moreover, given that $cPLA_2\alpha$ and $iPLA_2$ are the predominant PLA_2 messages in spinal cord (Karin Killermann et al., 2005), and *S*-isomers and *R*-isomers of BEL were reported to be more selective for $iPLA_2\beta$ and $iPLA_2\gamma$, respectively (Jenkins et al., 2002), we speculate that the α isoform of $cPLA_2$ may be involved mainly in the injury-induced LPA synthesis, but the detailed subtype of $iPLA_2$ involved in this study is still unclear. Using the specific inhibitor or antisense oligodeoxynucleotide for each